every mixture was made separately it could also be possible that one of the chemicals used to prepare the BGE or the FMOC itself was contaminated which resulted in those impurity peaks. To determine if the chemicals were contaminated the next run will be prepared with a different batch of chemicals.

Trp was observed with a relatively low signal intensity, this was in accordance with previous results from Figure 11 where Trp was also observed with a signal intensity which was lower than expected. When the emission spectra of Trp was compared with the emission spectra of the other amino acids it was observed that Trp was the only amino acid with a different emission spectra. The λmax of FMOC-Trp was 360 nm and the λmax of the other FMOC-amino acids was 330 nm , which explains the lower signal intensity because the electropherogram was taken at 330±10 nm. It was unknown why Trp was the only FMOC-amino acid with a different emission spectra compared to the other FMOC-amino acids.

The enantiomers of Ala and Pro were observed but they were both not baseline separated. Pro had relatively broad peaks compared to the other amino acid peaks, the reason for this was unknown. Gln, Thr and Tyr migrated very close to the FMOC peak which resulted with some of the enantiomers to partly or completely overlap with the FMOC peak. This might be solved by changing the concentration of SDS in the BGE so the interaction of the amino acids with the BGE changes and thus the migration times. Only one peak was observed of Gly, which was expected since Gly doesn't have a chiral center and therefore no enantiomers.

His, Arg, Asn, Ser, Cys and Lys were not observed after 90 minutes of measuring. In the past Cys and Lys were sometimes observed by the previous student, it was hypothesized that these amino acids had a strong interaction with SDS and therefore retained longer. When looking at the structural formula of Lys and Cys there are two possible binding locations for the FMOC (see Figure 16). It might have been possible that both binding locations were derivatized which would have lead to more interaction with the SDS micelles and therefore a longer migration time. It was believed that the reason that the previous student sometimes observed Cys or Lys was because it might be possible that only one binding side was derivatized with some runs. Fradi et al. [10] did also not observe Cys or Lys.It was unknown why Ser, Arg, His and Asn were unobserved. It might be possible that those amino acids overlap with the FMOC impurities.

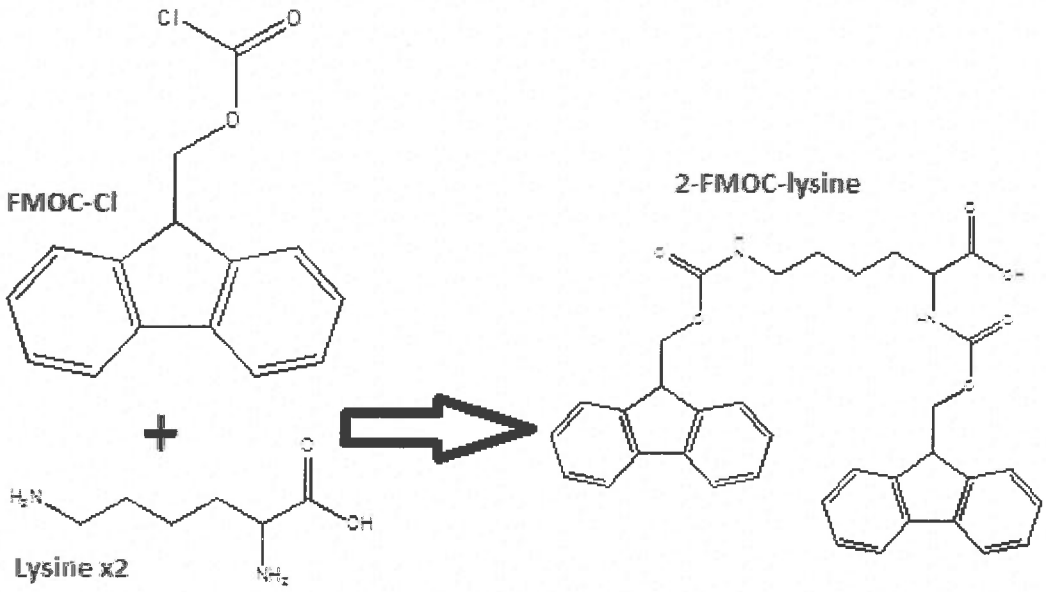

Figure 16: Derivatization reaction of lysine with FMOC on 2 binding locations

Amino acid mixture

Based on the migration times an estimation was made on which amino acids could be measured together and which ones might overlap with each other. It was hypothesized that Tyr, Pro and Ala overlap with each other with at least one enantiomer. Met and Val would most likely overlap with one enantiomer, as well as Ile and Leu. Based on the migration times it was hypothesized that either Met, Ile, Phe, Glu and Asp or Val, Ile, Phe, Glu and Asp could be measured together in a mixture and successfully enantioseparate without overlapping.
The CE method for in-line derivatization was used to enantioseparate all the mixtures. First Met and Ile were measured because this mixture was also measured in the previous experiment. These two amino acids were also used to indicate if a measurement was successful. If a similar migration time and peak intensity combined with similar FMOC peaks was obtained as was previously measured for Met and Ile, the run was deemed successful. After that Glu, Asp and Phe were added to the mix one at a time.

See Figure 17 for the results.

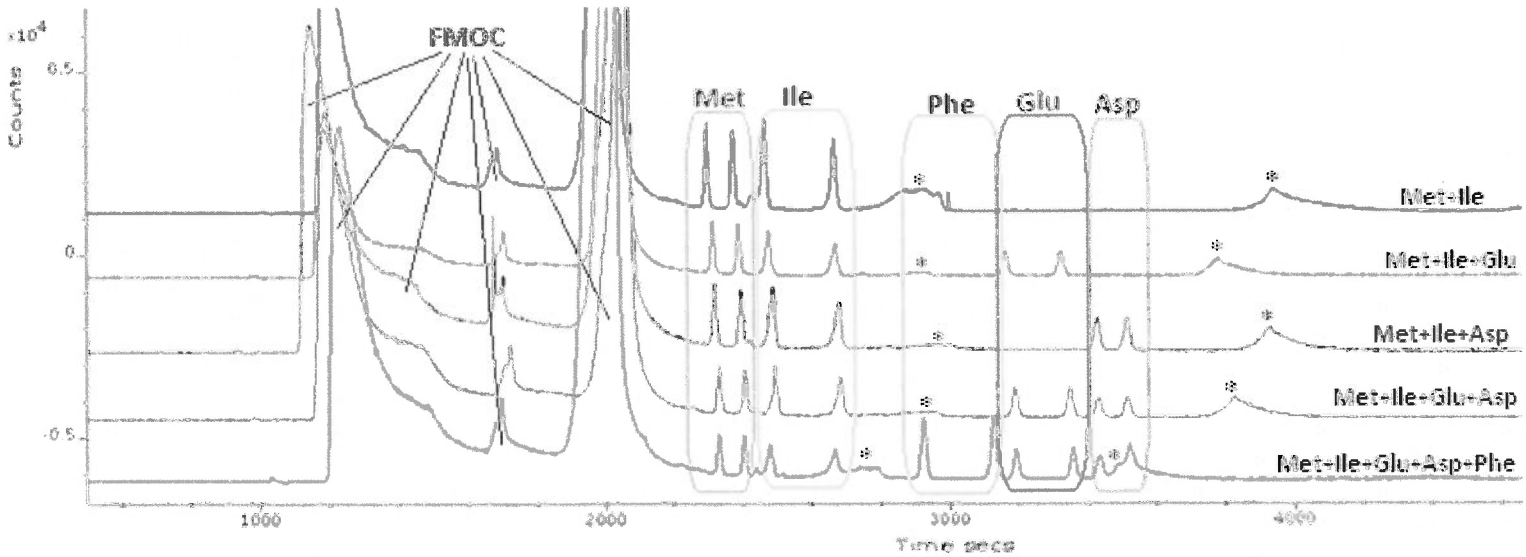

Figure 17: Electropherograms of the in-line derivatized mixture of Met, Ile, Phe, Glu & Asp in multiple steps. From top to bottom respectively: Met+Ile | Met+Ile+Glu | Met+Ile+Asp | Met+Ile+Glu+Asp | Met+Ile+Glu+Asp+Phe.
All runs had the same FMOC peaks but not all FMOC peaks were marked to maintain visibility.
Peaks marked with a * were impurities

All runs had a similar FMOC peak formation and were deemed successful according to the criteria stated in the beginning of this experiment. Some impurities (peaks marked with a *) with different migration times were observed while the migration times of the amino acids did not visually change between the runs.
All amino acids in all runs were enantioseparated without any overlap.

The Impurities (peaks marked with a *) at circa t=2800 and t=3900 seconds were most likely impurities and were also observed in the results from Figure 14. Since these runs were made with a different batch of chemicals than the runs from Figure 14 it could be concluded that the impurities were not due to contamination of the chemicals. It was believed these impurities originated from the FMOC. These impurities were not observed when an amino acid was measured without FMOC or when measuring off-line derivatized amino acids (see Figure 8 and Figure 12). With off-line derivatization the FMOC was extracted with pentane after the derivatization, the possibility existed that only with a relatively high concentration of remaining FMOC these impurities would be observed.

The impurities overlap with the amino acid peaks in the bottom run in Figure 17 at t=2700 and t=3500 seconds. The migration times of these impurities were shorter compared to the other impurities (circa t=2900 and t=3800/3900 seconds). It was unknown what could've caused this difference.

The amino acid mixture of Met, Ile, Glu, Asp and Phe was successfully enantioseparated without any overlap with each other. The enantiomers were also baseline separated and by adding the amino acids one by one it was easy to observe which peaks belonged to which amino acid. Visually observed none of the enantiomers show a shift in migration time between runs which indicates the results are repeatable.

5.3 Optimization

As more amino acids were added to the mix, the concentration of each enantiomer got lower because a total concentration of 500 µM was used. It was observed that due to the lower concentration the peak intensities of the enantiomers got lower as well. A hypothesis was made that using a capillary with a 75 µM internal diameter might improve the sensitivity compared to the current capillary which has an internal diameter of 50 µM. This hypothesis was based on the idea that a larger internal diameter increases the path length, and according to the Beer-Lambert law (see Figuur 18) increasing the path length increases the absorbance. It was reasoned that an increase of absorbance also resulted in an increase of fluorescence.

$$E = \varepsilon \cdot c \cdot L$$

Figuur 18: Formula of the Beer-Lambert law where E is the absorbance, ε is the molar attenuation coefficient, c is the concentration and L is the path length.

50µm ID capillary VS 75µm ID capillary

To possibly improve the sensitivity it was determined which capillary, the 50µm ID or the 75µm ID, results in a better signal to noise ratio. To determine this Met and Phe were measured in a mixture using a 50µm ID capillary and a 75µm ID capillary with both UV detection and fluorescence detection. The CE method for in-line derivatization was used to enantioseparate the mixture. See Table 8, Table 9, Table 10 and Table 11 for the results.

Table 8: Overview of the signal and noise values of the UV measurement using a 50µm ID capillary

UV measurement - 50µm ID capillary				
	D-Met	L-Met	D-Phe	L-Phe
noise	0.00002	0.00002	0.00003	0.00003
signal	0.001235	0.001037	0.002422	0.00238
S/N	61.75	51.85	80.73333	79.33333

Table 9: Overview of the signal and noise values of the fluorescence measurement using a 50µm ID capillary

Fluorescence measurement - 50µm ID capillary				
	D-Met	L-Met	D-Phe	L-Phe
Noise	5	5	6	7
Signal	1314	1020	2105	2298
S/N	263	204	351	328

Table 10: Overview of the signal and noise values of the UV measurement using a 75µm ID capillary

UV measurement - 75µm ID capillary				
	D-Met	L-Met	D-Phe	L-Phe
noise	0.00002	0.00002	0.00003	0.00003
signal	0.001436	0.001507	0.002892	0.002541
S/N	72	75	96	85

Table 11: Overview of the signal and noise values of the fluorescence measurement using a 75µm ID capillary

Fluorescence measurement - 75µm ID capillary				
	D-Met	L-Met	D-Phe	L-Phe
Noise	11	7	10	8
Signal	31175	27223	30021	29394
S/N	2834	3889	3002	3674

The S/N ratios of the UV measurements using a 50 and 75µm ID capillary were not regarded as different from each other.
When comparing the S/N ratio of fluorescence and UV using a 50µm ID capillary the S/N ratios of the fluorescence measurements were circa 4 times higher than the UV measurements.
The S/N ratios of the fluorescence measurements using a 75µm ID capillary was circa 10 times higher than the fluorescence measurements using a 50µm ID capillary.

The relatively low increase in sensitivity from UV to fluorescence detection using a 50µm ID capillary was unexpected. Theoretically fluorescence is more or less 100 times more sensitive and we expected an increase of circa 80 to 100 times when we switched from UV to fluorescence, but with this capillary and setup the increase in sensitivity was 4 times. It was believed this was due to the detector cell not being able to utilize all the light from the excitation source because of light scattering. Since the capillaries are round it was possible that a lot of light was scattered and lost and that only a small portion actually enters the capillary to excite the sample.
The fluorescence measurement using a 75µm ID capillary had a 10 times increase in S/N compared to the 50µm ID capillary fluorescence measurement. This difference between S/N ratios between 75µm and 50µm ID capillary with fluorescence detection was most likely due to the bigger capillary which enables more light to enter the capillary and therefore less light was scattered and lost.
This means that the hypothesis of increasing the signal by increasing the internal diameter of the capillary was correct.

With the 75μM ID capillary the S/N ratios of fluorescence were circa 40 times higher than the S/N ratios of UV. Although this increase was still lower than we initially thought, the increase was higher compared to the switch from UV to fluorescence with the 50μM capillary. From now on the 75μm ID capillary was used for all experiments.

Amino acid mixture

The amino acid mixture of Met, Ile, Phe, Asp and Glu was measured again due to the change of the capillary from 50μm to 75μm ID. Additional amino acids were also added to the mixture to determine if the mixture could be expanded.

The CE method for in-line derivatization was used to enantioseparate all the mixtures. First Ile was measured and then the other amino acids were added to the mixture one at the time (Met, Phe, Glu and Asp). This was done to make sure it could've been observed if the migration order changed due to the change to a 75μM ID capillary instead of a 50μM ID capillary. After the first run, Ile was also used as a reference to indicate if a measurement was successful. If a similar migration time and peak intensity combined with similar FMOC peaks were obtained as was previously measured for Ile, the run was deemed successful. After that Leu, Val, Ala, Gly and Pro were added to the mixture one at a time. These amino acids were chosen based on previous results where those amino acids were observed and could possibly be added to the mixture without overlap with other amino acids.

See Figure 19 and Figure 20 for the results.

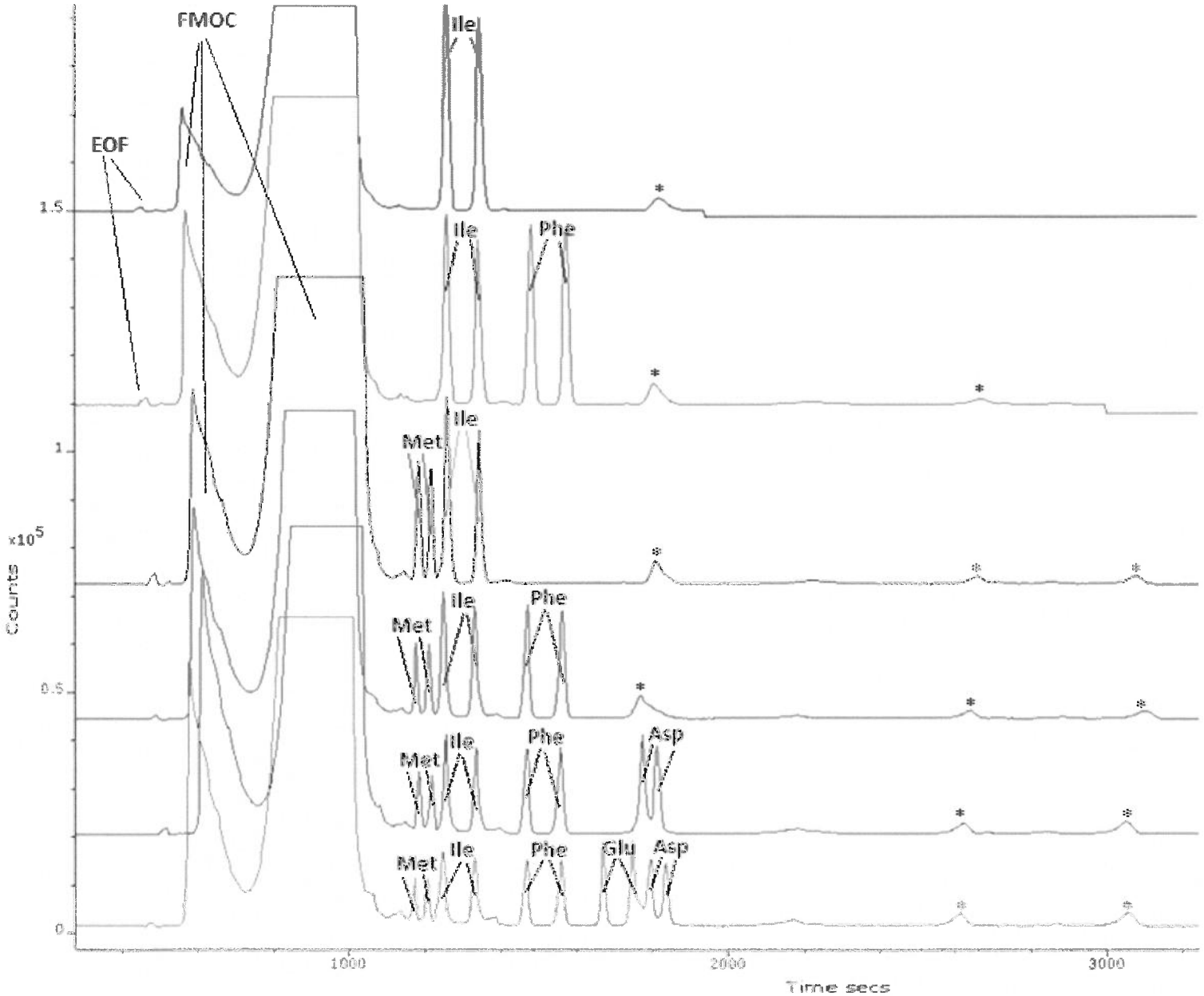

Figure 19: Electropherograms of the in-line derivatized mixture of Met, Ile, Phe, Glu & Asp in multiple steps. From top to bottom respectively: Ile | Ile+Phe | Met+Ile | Met+Ile+Phe | Met+Ile+Phe+Asp | Met+Ile+Phe+Glu+Asp.
All runs had the same EOF and FMOC peaks but not all those peaks were marked to maintain visibility.
Peaks marked with a * were impurities

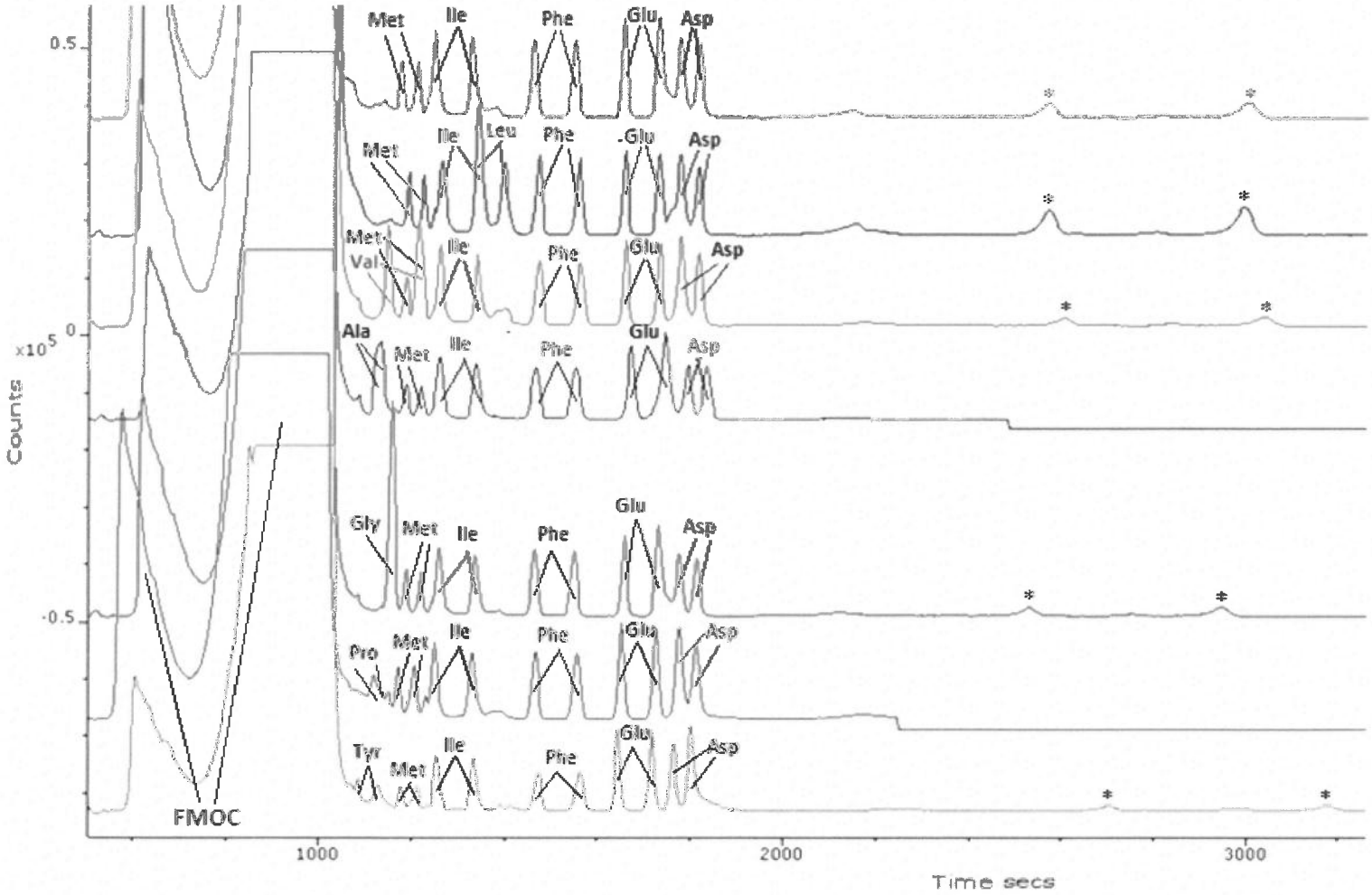

Figure 20: Electropherograms of the in-line derivatized mixture of Met, Ile, Phe, Glu & Asp + others. From top to bottom respectively: Met+Ile+Phe+Glu+Asp | Met+Ile+Phe+Glu+Asp+Leu | Met+Ile+Phe+Glu+Asp+Val | Met+Ile+Phe+Glu+Asp+Ala | Met+Ile+Phe+Glu+Asp+Gly | Met+Ile+Phe+Glu+Asp+Pro | Met+Ile+Phe+Glu+Asp+Tyr.
All runs had the same FMOC peaks but not all those peaks were marked to maintain visibility.
Peaks marked with a * were impurities

All runs had a similar FMOC peak formation and were deemed successful according to the criteria stated in the beginning of this experiment. Different FMOC peaks were observed compared to previous results (Figure 12, Figure 14, Figure 17).
Peaks marked with an * were impurities.

When Leu was added to the mixture D-Leu overlapped with L-Ile, whileL- Val overlapped with L-Met when it was added to the mixture. Ala was observed as one peak, for Gly one relatively large peak was observed. For both Pro and Tyr two peaks were observed.

D-Leu overlapped with L-Ile, while L-Val overlapped with L-Met when it was added to the mix. This confirmed the hypothesis in previous experiment regarding the estimation of amino acids suitable for the mix. The peaks were identified through spiking.

The relatively large peak from Gly was as expected due to Gly lacking a chiral center thus having no enantiomers, this resulted in a two times higher concentration of Gly compared to the other entantiomers in the same sample.

Two peaks of Pro were observed but they were not baseline separated from each other. The two enantiomers of Tyr were observed and enantioseparated, the peaks were close to the FMOC peak. Because of this Tyr overlapped with the end of the FMOC peak, this might cause deviating signal intensities of the Tyr enantiomers in future runs. Despite this drawback, Tyr was successfully enantioseparated in the mixture.

The migration order of the amino had not changed but an overall decrease in migration times was observed compared to the results from previous experiments. This was as expected because the larger internal diameter of the capillary of 75μM allows a higher flow.

Temperature

To potentially add more amino acids to the mixture it was necessary to determine which parameters could be changed to increase our migration window or change the migration order. It was believed that the migration window could be influenced by changing the temperature and that the migration order could be influenced through the SDS concentration. It was also hypothesized that the overlap of Thr, Gln and Tyr with the FMOC peak (Figure 13, Figure 15 and Figure 20), could be prevented by reducing the FMOC peak width. The effect of the temperature was determined first.
The CE method for in-line derivatization was used to enantioseparate the mixture of Met, Ile, Phe, Glu, Asp & Tyr 5 times. For each measurement a different temperature was used, 20 - 22 - 25 - 27 - 30 °C.
See Figure 21 and Table 12 for the results.

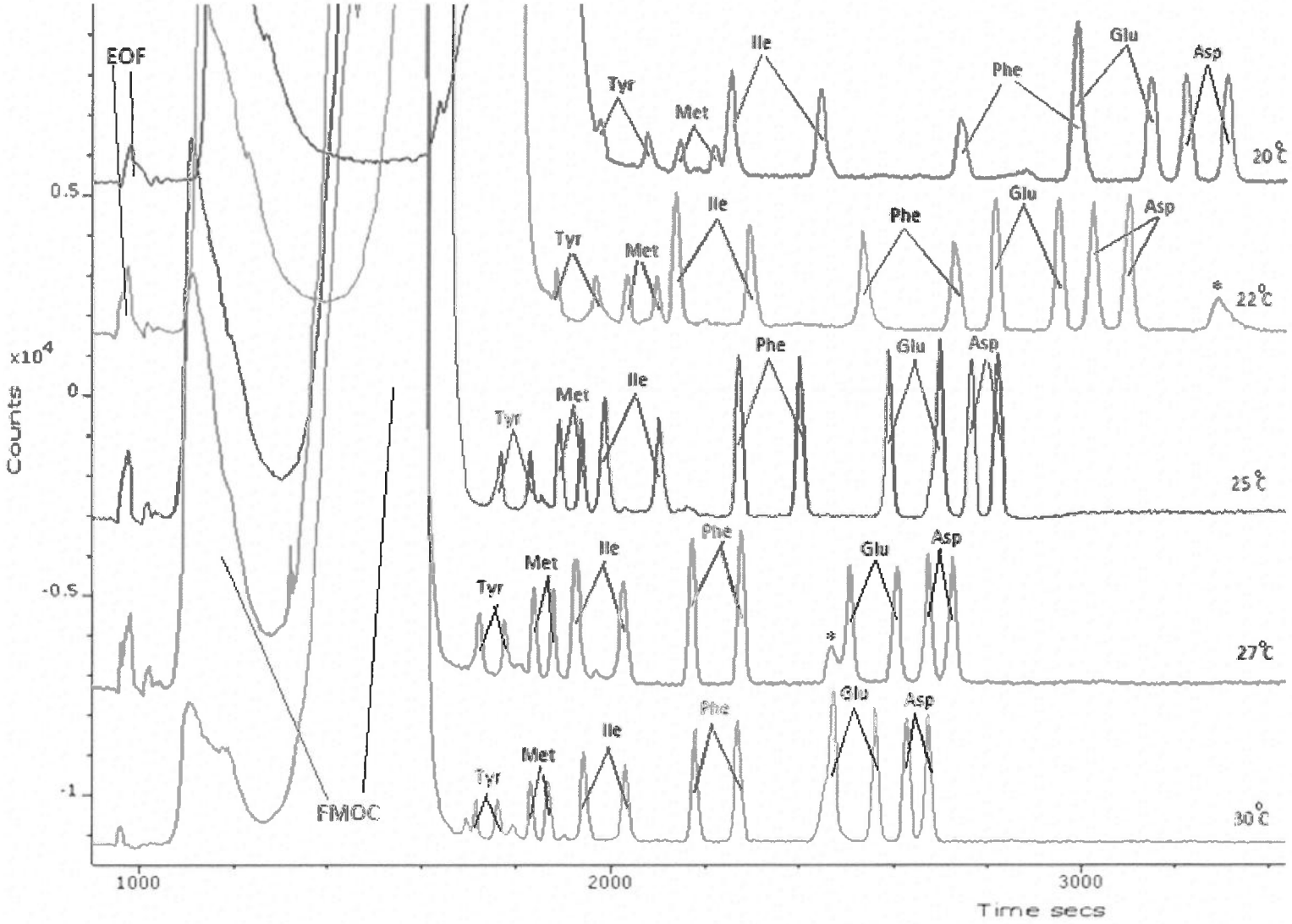

Figure 21: Electropherograms of the in-line derivatized mixture of Met, Ile, Phe, Glu, Asp & Tyr with different temperatures. From top to bottom 20 - 22 - 25 - 27 - 30 °C respectively.
All runs had the same EOF and FMOC peaks but not all those peaks were marked to maintain visibility.
Peaks marked with a * were impurities

Table 12: Overview of the resolution, migration time and S/N ratio's of all measured enantiomers at 20, 22, 25, 27 and 30 °C. The R_s value of each enantiomer was based on the first peak left of it.
The underlined enantiomers overlapped with each other.

20°C			
Peak	R_s	MT (s)	S/N
FMOC	-	1910	-
D-Tyr	0.1	1987	52
L-Tyr	3.5	2087	70
D-Met	2.1	2157	76
L-Met	2.2	2230	64
D-Ile	0.9	2266	174
L-Ile	3.4	2457	172
D-Phe	4.7	2749	98
L-Phe	3.8	3000	302
D-Glu			
L-Glu	2.5	3158	222
D-Asp	1.3	3231	232
L-Asp	1.5	3322	240

22°C			
Peak	R_s	MT (s)	S/N
FMOC	-	1780	-
D-Tyr	0.5	1887	60
L-Tyr	2.2	1972	72
D-Met	1.5	2036	92
L-Met	1.6	2096	86
D-Ile	1.1	2139	198
L-Ile	3.2	2297	168
D-Phe	4.2	2536	140
L-Phe	3.2	2727	122
D-Glu	1.7	2818	216
L-Glu	2.6	2955	230
D-Asp	1.4	3025	228
L-Asp	1.4	3101	232

25°C			
Peak	R_s	MT (s)	S/N
FMOC	-	1580	-
D-Tyr	1.5	1783	74
L-Tyr	1.9	1831	78
D-Met	2.1	1907	122
L-Met	1.5	1966	124
D-Ile	1.4	1994	176
L-Ile	2.6	2112	168
D-Phe	3.1	2266	212
L-Phe	3.0	2408	210
D-Glu	4.3	2595	232
L-Glu	2.1	2710	256
D-Asp	1.5	2791	230
L-Asp	1.4	2895	237

27°C			
Peak	R_s	MT (s)	S/N
FMOC	-	1510	-
D-Tyr	1.5	1714	72
L-Tyr	1.6	1765	68
D-Met	1.9	1826	102
L-Met	1.4	1866	106
D-Ile	1.2	1914	142
L-Ile	2.0	2017	128
D-Phe	3.1	2163	166
L-Phe	2.3	2266	174
D-Glu	5.2	2500	140
L-Glu	1.9	2597	138
D-Asp	1.4	2663	150
L-Asp	1.1	2715	146

30°C			
Peak	R_s	MT (s)	S/N
FMOC	-	1530	-
D-Tyr	1.5	1710	54
L-Tyr	1.6	1735	56
D-Met	2.2	1825	92
L-Met	1.3	1862	90
D-Ile	1.9	1937	124
L-Ile	1.8	2025	108
D-Phe	2.9	2184	156
L-Phe	1.8	2275	162
D-Glu	3.2	2478	202
L-Glu	1.5	2566	194
D-Asp	1.5	2623	178
L-Asp	1.0	2679	184

All amino acids in all runs appeared to have been enantioseparated, but the enantiomers L-Phe and D-Glu overlap with each other during the run at 20°C (identified by spiking). All D-enantiomers migrated before their L-enantiomer counterpart. 2 impurities were observed (peaks marked with an *).
A trend was observed where an increase in the temperature resulted in the decrease of the total migration time of the run compared to a run with a lower temperature.
Different S/N ratio's were observed between the runs at different temperatures with the run at 25°C having the highest S/N ratio's on average.

A trend was observed where a lower temperature increases the overall migration time. L-Phe and D-Glu only overlapped with each other during the run at 20°C and the migration time of the EOF peak (circa t=980 seconds) did not shift in any run. This indicates that the temperature influences the interaction of the sample with the BGE and that temperature variations of this scale did not influence the electroosmotic flow. Based on the observation that L-Phe and D-Glu overlapped at 20°C, indicated that the amount of influence the temperature had on the interaction with the BGE, depended on the amino acid. This can also be observed in the R_s values of each enantiomer, for example L-Ile shifted from an R_s of 3.4 at 20°C to an R_s of 1.8 at 30°C, while D-Asp shifter from an R_s of 1.3 at 20°C to an R_s of 1.5 at 30°C.
An impurity was observed in 2 electropherograms (peaks marked with an *), since those peaks were not recurring in all runs it was unknown what the origin of these peaks were.

Based on the S/N ratios of the enantiomers it seemed that the run at 25°C had the highest S/N ratios compared to the runs at other temperatures. It was unknown if that was caused by the temperature or if it were variances between runs.

An R_s value of 1.5 is regarded as the minimum for baseline separation. When R_s values were compared it was observed that the run at 25°C had the least enantiomers below 1.5 with only 2 enantiomers having an R_s of 1.4.

By lowering the temperature it was possible to increase the migration window which might create the possibility to add another amino acid, but the R_s values of D-Tyr and D-Ile indicate those enantiomer will start to overlap with other peaks if the temperature will be lowered more. With L-Phe and D-Glu already overlapping with each other at 20°C it is unlikely to increase the migration window by lowering the temperature without losing any enantiomer due to overlap.

When comparing the R_s values and S/N ratios of the enantiomers of all the runs it was chosen that the temperature of 25°C gave the most optimal results and was continued to be used.

SDS concentration

A different option needed to be explored to add more amino acids to the mixture without overlap, such as the migration order which could be influenced through the SDS concentration as was discussed previously.
The CE method for in-line derivatization was used to enantioseparate the mixture 3 times. For each measurement a different SDS concentration was used, 25, 30 and 35 mM. This was done to determine the influence of the SDS concentration on the measurement of the amino acid mixture and to give an indication if it enables the addition of more amino acids to the mixture.
See Figure 22 for the results.

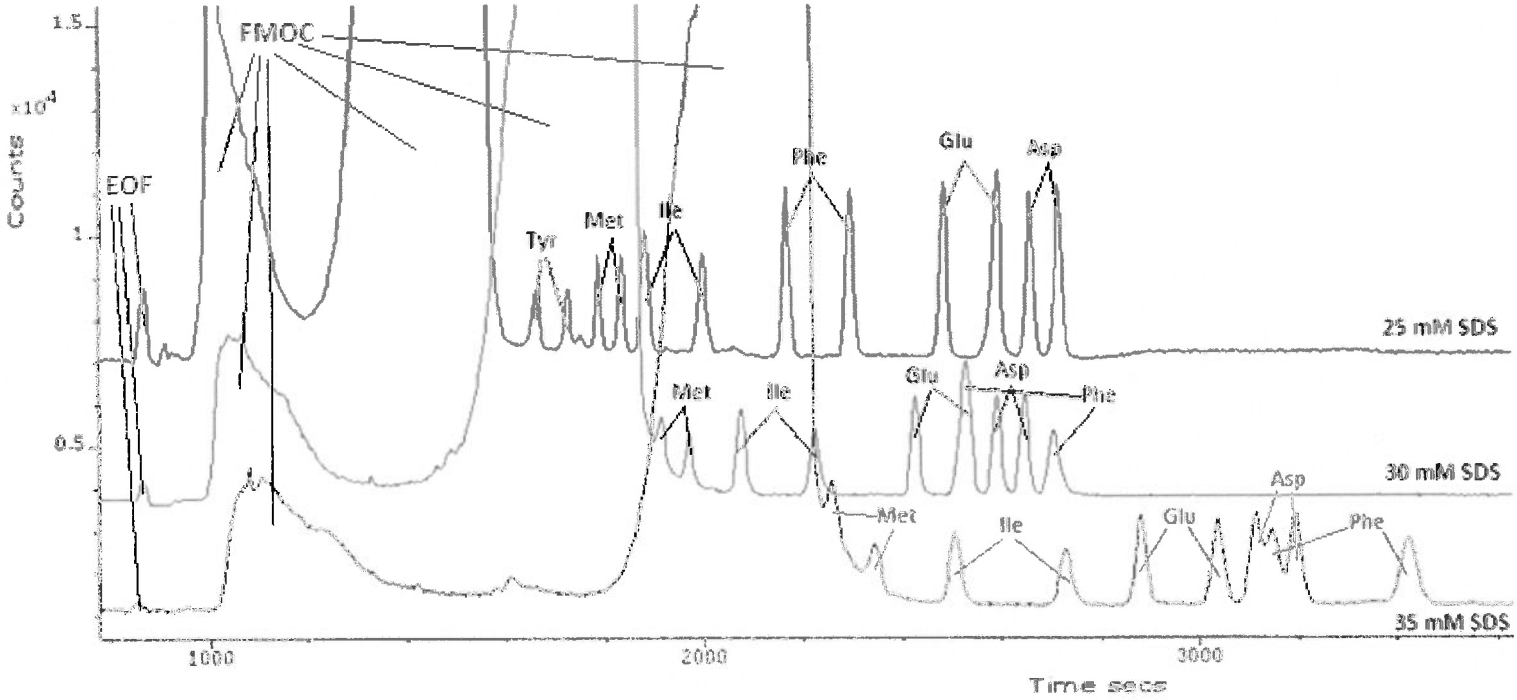

Figure 22: Electropherograms of the in-line derivatized mixture of Met, Ile, Phe, Glu, Asp & Tyr with different SDS concentrations. From top to bottom 25 - 30 - 35 mM SDS respectively

Tyr was not observed at the runs with 30 and 35 mM SDS. D-Phe overlapped with L-Glu at 30 mM SDS concentration, and with D- and L-Asp at 35 mM SDS concentration. Different migration times were observed between the runs with different SDS concentrations.

A trend was observed where a higher SDS concentration results in higher migration times as was expected due to the results of a similar experiment of different SDS concentration of a previous student. These results of the previous student were the reason only an increased SDS concentration was explored due to the knowledge that reducing the SDS concentration only shortens the total migration window which would reduce the amount of enantiomers that successfully enantioseparate without overlap.

The migration times of the EOF peak (circa t=870 seconds) did not change which indicates that the variations of the SDS concentration of this scale did not influence the electroosmotic flow.
Tyr was not observed at the runs with 30 and 35 mM SDS, it was believed the migration times of Tyr and the FMOC had shifted and the peaks overlapped. Met, Ile, Glu and Asp appeared to maintain the same migration order as was observed in previous experiments of Met-Ile-Phe-Glu-Asp. Only the enantiomers of Phe was observed in a different location of the usual migration order. With 30 mM SDS D-Phe and L-Glu overlapped with each other (circa t=2600 seconds) but at 35 mM SDS D-Phe overlapped with both D- and L-Asp (circa t=3100-3200 seconds). This indicated that Phe was more influenced by the SDS concentration compared to Tyr, Met, Ile, Glu and Asp. A reason for this could be that Phe is more hydrophobic than the other amino acids and therefore had more interaction with the SDS micelles.

Due to the fact that the enantiomers of Tyr overlapped with the FMOC and D-Met started to overlap with the FMOC as well with increased SDS concentrations, it was decided that increasing the SDS concentration was not a viable option to potentially add more amino acids to the mixture because multiple enantiomers would not be observed.

FMOC peak width

The potential amino acids Ala, Gln and Thr all migrated close to the FMOC and partially overlap with it. It was hypothesized that those amino acids might successfully be enantioseparated without overlap in the mixture if the FMOC peak width was reduced.
With this experiment it was determined if it was possible to reduce the FMOC peak width.
The CE method for in-line derivatization was used to enantioseparate the mixture with different concentrations of FMOC and different injection times. Runs were made with a FMOC concentration of 2.5 - 2.0 - 1.5 - 1.0 - 0.5 mM FMOC to determine the influence of the FMOC concentration on the FMOC peak width. Additional runs were made where 2.5 mM FMOC was used with injection times of 24 - 20 - 16 - 12 - 8 seconds and 5 mM FMOC was used with injection times of 24 - 16 - 8 - 6 - 4 seconds to determine the influence of the injection time on the FMOC peak width.
See Figure 23, Figure 24, Figure 25 for the results.

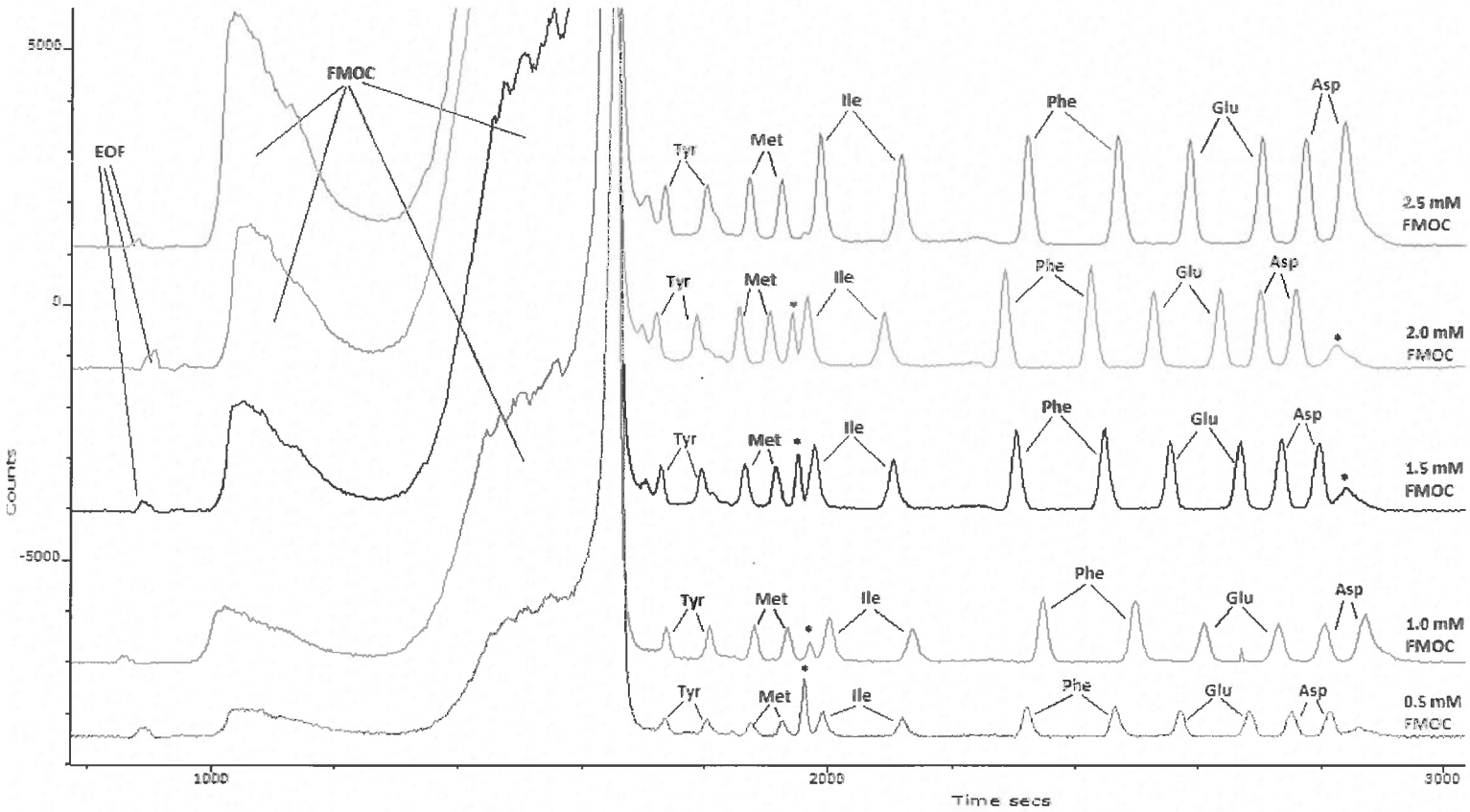

Figure 23: Electropherograms of the in-line derivatized mixture of Met, Ile, Phe, Glu, Asp & Tyr with different FMOC concentrations injected for 24 seconds (0.3 psi). From top to bottom 2.5 - 2.0 - 1.5 - 1.0 - 0.5 mM FMOC respectively. All runs had the same EOF and FMOC peaks but not all those peaks were marked to maintain visibility.
Peaks marked with a * were impurities

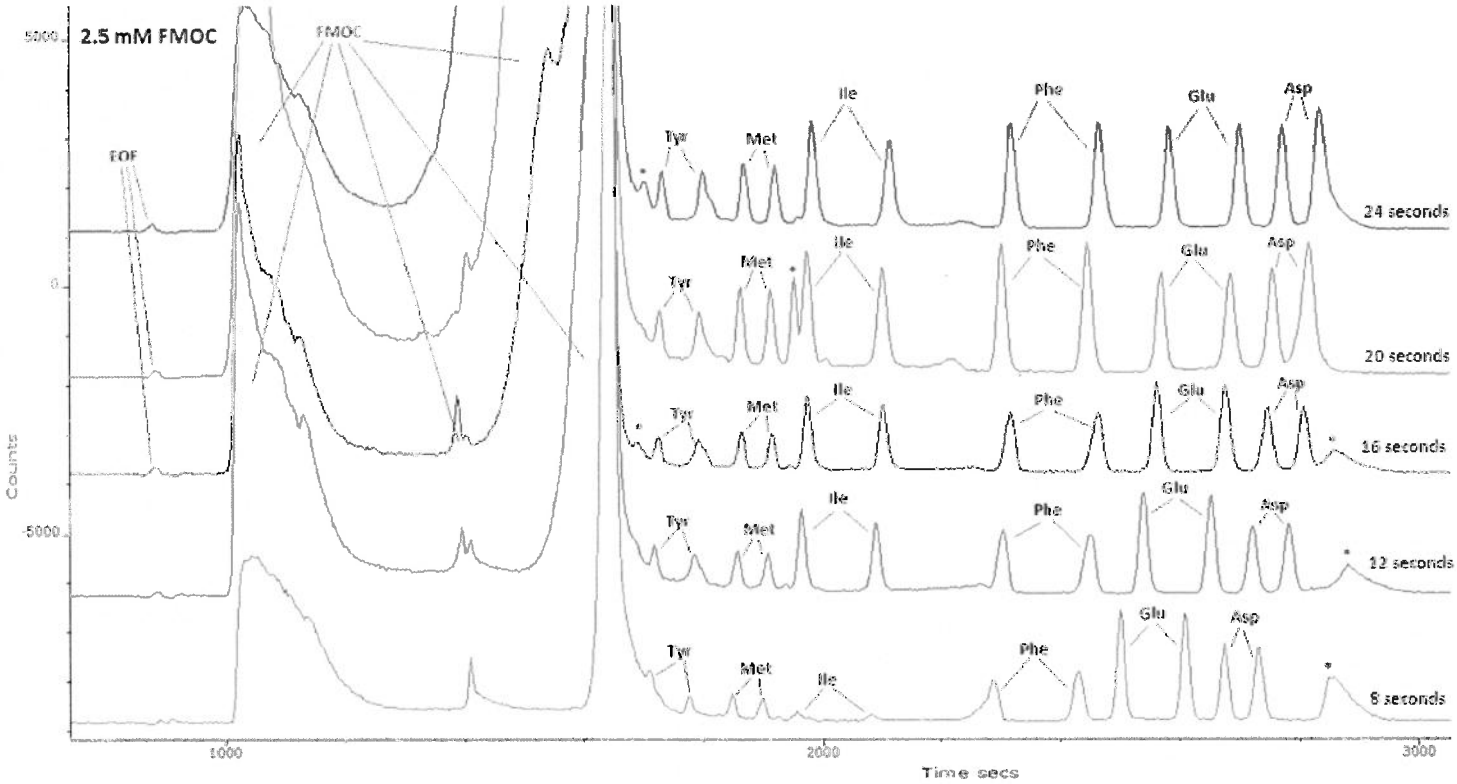

Figure 24: Electropherograms of the in-line derivatized mixture of Met, Ile, Phe, Glu, Asp & Tyr with different FMOC injections at 2.5 mM at 0.3 psi. From top to bottom 24 - 20 - 16 - 12 - 8 seconds FMOC injection respectively. All runs had the same EOF and FMOC peaks but not all those peaks were marked to maintain visibility. Peaks marked with a * were impurities

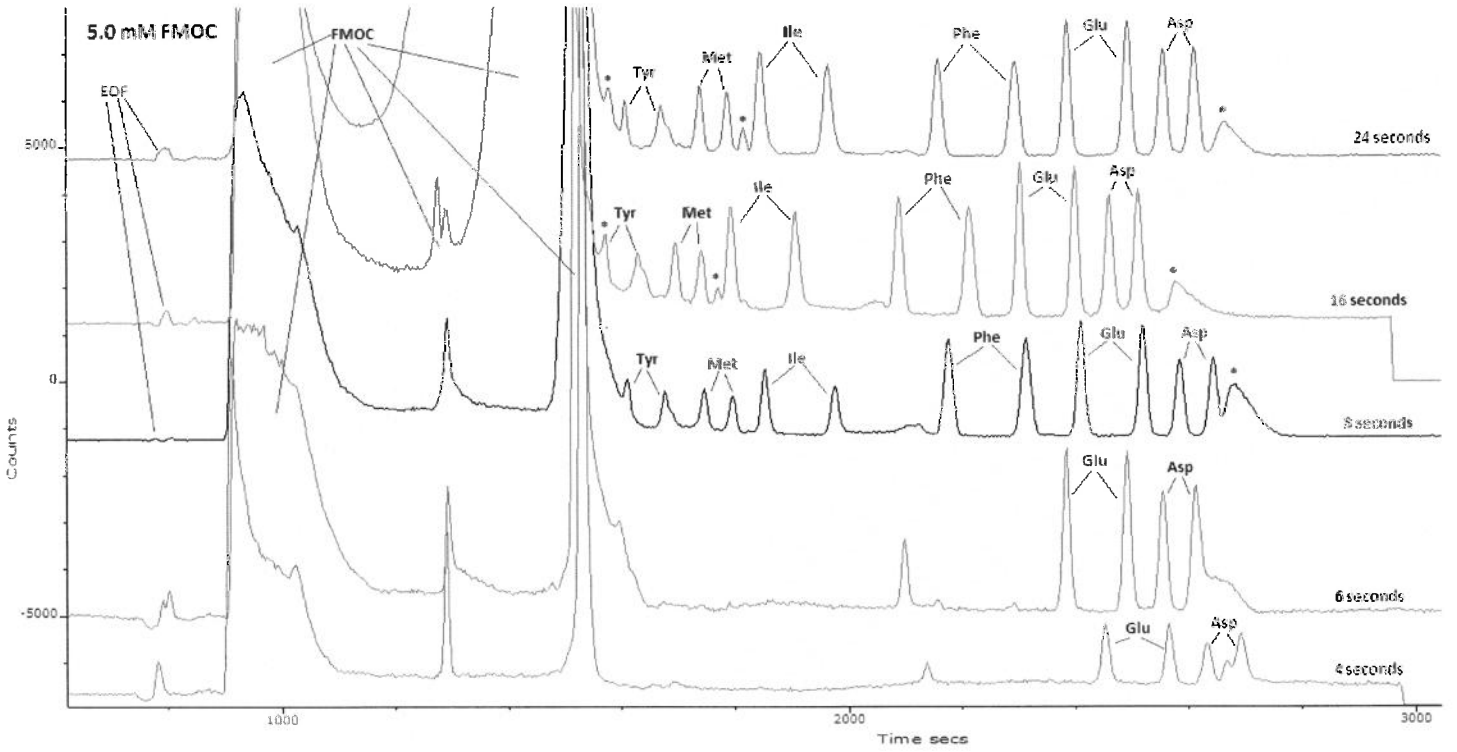

Figure 25: Electropherograms of the in-line derivatized mixture of Met, Ile, Phe, Glu, Asp & Tyr with different FMOC injections at 5.0 mM at 0.3 psi. From top to bottom 24 - 16 - 8 - 6 - 4 seconds FMOC injection respectively. All runs had the same EOF and FMOC peaks but not all those peaks were marked to maintain visibility. Peaks marked with a * were impurities

In Figure 23 there was visually no change in the FMOC peak width observed. In both Figure 24 and Figure 25 it was observed that the FMOC peak width decreased with a lower injection volume of FMOC.
A decrease in signal intensity was observed with the 8 seconds injection in Figure 24. Tyr, Met, Ile and Phe were not observed with the 6 and 4 seconds injection in Figure 25. Besides those all other amino acids were successfully observed and enantioseparated.
Peaks marked with an * were impurities.

There was visually no change in the FMOC peak width observed in Figure 23, this indicated that the concentration of the FMOC did not influence the width of the FMOC peak at these concentrations. This was most likely due to the relatively high injection volume of 24 seconds which would result in a large plug length. It was believed that the larger the plug length, the more time it takes to pass the detection window, and therefore a broader peak.
In Figure 24 and Figure 25 a trend was observed where the lower the injection time was, the smaller was the width of the FMOC peak. It was believed that a smaller FMOC peak might enable the enantioseparation of other amino acids. For example Thr, which overlapped with the FMOC in previous experiments.

In Figure 24 a decrease in S/N ratios could be visually observed for Tyr, Met, Ile and Phe when the injection time got lowered to 8 seconds. This was as expected because a lower injection time results in less FMOC injected for the derivatization which reduces the derivatization yield. Tyr, Met, Ile and Phe were not observed with the 6 and 4 seconds injection in Figure 25. The reason for this was also most likely the lower amount of FMOC due to the decreased injection volume. This probably resulted in an incomplete derivatization of the amino acid mixture.
Glu and Asp were still observed with the 6 and 4 seconds injection in Figure 25. This might indicate that the reaction rate of the derivatization of Glu and Asp is higher than that of Tyr, Met, Ile and Phe. It might be possible that a higher concentration of FMOC and lower injection time could result in a successful enantioseparation of the mixture without reducing the derivatization yield.

A new experiment need to be performed to determine how the best results could have been obtained by changing the FMOC concentration and injection time without losing sensitivity.

FMOC concentration and injection time

The goal of this experiment was to determine the most optimal FMOC concentration and injection time to reduce the FMOC peak width as much as possible while maintaining sensitivity. This was done because it was important not to lose any sensitivity for the sake of reducing the FMOC peak width.

An injection time of 6 seconds with a FMOC concentration of 10 and 15 mM was already tested but the results were similar as was observed in Figure 25 with the 6 and 4 seconds injection time. The amino acid mixture was not successfully enantioseparated with those parameters because multiple amino acids were missing. Therefore it was believed that the 8 seconds injection time was the most optimal injection time while reducing the FMOC peak width. Now the different FMOC concentrations were tested with the 8 seconds injection.

The CE method for in-line derivatization was used to enantioseparate the mixture with different concentrations of FMOC and 8 seconds of injection time. Runs were made with a concentration of 5.0 - 7.5 - 10 - 15 mM FMOC and the S/N ratios of L-Met, L-Phe and L-Asp were compared with each other to determine which FMOC concentration obtained the best S/N ratios.

The enantiomers L-Met, L-Phe and L-Asp were chosen for the comparison because they were relatively spread out in the migration window. Also, based on previous results in this study, these peaks often had good baseline separation which made the S/N ratio more accurate.

See Table 13 for the results.

Table 13: Overview of the obtained S/N ratios of L-Met, L-Phe and L-Asp from the in-line derivatized amino acid mixture with different FMOC concentrations and 8 seconds injection time (0.3 psi)

	L-Met			L-Phe			L-Asp		
	Noise	Signal	S/N	Noise	Signal	S/N	Noise	Signal	S/N
5 mM FMOC	2.4	360	150	1.6	690	431	1.5	165	110
7.5 mM FMOC	4	600	150	2	1047	524	2	303	152
10 mM FMOC	3.2	701	219	3.4	1790	575	2	403	202
15 mM FMOC	5	742	148	1.6	690	526	5	546	109

All amino acids were successfully observed and enantioseparated in all runs described in Table 13. The best signal to noise ratios for all three enantiomers were obtained while using 10 mM FMOC with 8 seconds injection (0.3 psi).

The S/N ratios obtained for L-Met and L-Phe are circa 1.5 to 2 higher than the S/N ratio's obtained with experiment 0 while using 10 mM FMOC with 8 seconds injection. For Figure 12 an FMOC concentration of 2.5 mM with 24 seconds injection time was used, which means that the total amount of FMOC injected was less compared to the 8 seconds injection of 10 mM FMOC in this experiment. With the shorter injection time of 8 seconds, the FMOC plug in the capillary would also be smaller. It was hypothesized that due to this smaller but more concentrated FMOC plug, the derivatization yield was increased which resulted in the increased S/N ratios.

With these new parameters, it is still uncertain if a new amino acid could be added to the mixture. With this increase in S/N ratios it might be possible that by optimizing other parameters the sensitivity could be increased even more. Such as the amino acid injection time, buffer injection time, the mixing voltage duration and ramp times.

Amino acid injection time

The amino acid injection time was also optimized because it was believed that a higher amino acid injection could potentially result in a higher sensitivity.
The CE method for in-line derivatization was used to enantioseparate the mixture with different amino acid injection times. Runs were made with an injection time of 12 - 10 - 8 - 6 seconds at 0.3 psi and the S/N ratios of L-Met, L-Phe and L-Asp were compared with each other to determine which injection time obtained the best S/N ratios.
The enantiomers L-Met, L-Phe and L-Asp were chosen for the comparison because they were relatively spread out in the migration window. Also, based on previous results in this study, these peaks often had good baseline separation which made the S/N ratio more accurate.

See Table 14 for the results.

Table 14: Overview of the obtained S/N ratios of L-Met, L-Phe and L-Asp from the in-line derivatized amino acid mixture with different amino acid injections at 0.3 psi

	L-MET			L-PHE			L-ASP		
AA injection	Signal	Noise	S/N	Signal	Noise	S/N	Signal	Noise	S/N
12 seconds	504	1.4	360	1028	1.1	935	288	1.4	206
10 seconds	680	1.6	425	1258	0.9	1398	436	1.7	256
8 seconds	556	1.4	397	1006	1.2	838	362	1.5	241
6 seconds	281	1.4	201	1016	1.8	564	263	1.7	155

All amino acids were successfully enantioseparated and observed in all runs.
The best signal to noise ratios for all three enantiomers were obtained while using an amino acid injection of 10 seconds at 0.3 psi.

The 8 seconds injection of the amino acids was also used in previous experiments and therefore similar S/N ratios were expected. The obtained S/N ratios of this experiment are circa 1.5 times higher than the ratios obtained when the capillary was switched to 75μm ID. It was hypothesized that this increase in S/N ratios was due to the change of capillary in between these experiments. When the capillary is changed, the capillary cell needs to be rebuild. The building of the cell requires a small amount of glycerol near the cell window (see 3.2 Fluorescence detection) which has a large influence on the sensitivity. It was believed that the capillary used for this experiment was slightly better build that the capillary that was used when the 75μm ID capillary was first installed.

The S/N ratios obtained by using an amino acid injection of 10 seconds at 0.3 psi were the highest compared to the other runs. It was expected that a higher injection time would result in a higher signal, but it was observed that an injection time of 12 seconds resulted in lower S/N ratios compared to an injection time of 10 seconds. It was hypothesized that an amino acid injection time of 12 seconds or higher would broaden the amino acid peaks due to the increased plug length. This would result in a decrease of the S/N ratios compared to a run with an amino acid injection time of 10 seconds. Therefore it was believed that the amino acid injection time of 10 seconds was the most optimal.

It was also believed that by optimizing other parameters the sensitivity could be increased even more. As was discussed before, the effects of the buffer injection time, the mixing voltage duration and ramp times should also be determined.

Buffer injection time

To determine the optimal buffer injection time the CE method for in-line derivatization was used to enantioseparate the mixture with different buffer injection times. Runs were made with a buffer injection time of 28 - 24 - 20 - 16 - 12 - 8 - 4 - 0 seconds at 0.3 psi and the S/N ratios of L-Met, L-Phe and L-Asp were compared with each other to determine which buffer injection time obtained the best S/N ratios.
The enantiomers L-Met, L-Phe and L-Asp were chosen for the comparison because they were relatively spread out in the migration window. Also, based on previous results in this study, these peaks often had good baseline separation which made the S/N ratio more accurate.

See Table 15 for the results.

Table 15: Overview of the obtained S/N ratios of L-Met, L-Phe and L-Asp from the in-line derivatized amino acid mixture with different buffer injection times at 0.3 psi

	L-MET			L-PHE			L-ASP		
buffer injection	Signal	Noise	S/N	Signal	Noise	S/N	Signal	Noise	S/N
28 seconds	632	3.1	204	1290	2.1	614	454	2.9	157
24 seconds	558	2.8	199	1073	1.9	565	539	2.6	207
20 seconds	1001	2.6	385	2412	1.8	1340	1888	2.3	821
16 seconds	856	2.2	389	2270	1.6	1419	2078	2.3	904
12 seconds	789	2.0	395	1376	1.5	917	828	1.9	436
8 seconds	1022	1.8	568	2198	1.5	1465	1115	1.7	656
4 seconds	1174	1.7	691	2210	1.2	1842	1014	1.4	724
0 seconds	1432	1.3	1102	2327	1.2	1939	1070	1.1	973

All amino acids were successfully observed and enantioseparated in all runs.
Based on results from Table 15 the amount of noise decreases when reducing the buffer injection time. The signal seemed visually higher with a buffer injection of 20 seconds or lower compared to the 28 and 24 seconds injection. Overall the S/N ratios increases when the buffer injection time was reduced.
The highest S/N ratios was obtained with 0 buffer injection time.

It was observed that the amount of noise decreases when the buffer injection time was reduced, this indicates that the buffer influences the baseline. For L-Met and L-Phe an increase in signal was also observed when the buffer injection time was reduced. This resulted in a 2 to 5 times increase in the S/N ratios compared to the results from Table 14.
The increase in signal with no buffer compared to 28 seconds of buffer injection might be due to an increase in the derivatization yield. With no buffer plug between the amino acid and the FMOC plugs, the amino acid and FMOC plugs reach each other faster. This could means there was less diffusion of the plugs in the capillary which might have increased the derivatization yield. The higher signal combined with the reduced noise resulted in better S/N ratios.

Theoretically the function of the sodium tetraborate buffer plug was for the deprotonation of the amino acids which would help the derivatization reaction. But it was hypothesized that because the amino acids were dissolved in the same buffer solution that was used for the buffer plug, the conditions were the same for the amino acids with or without the buffer plug. And therefore it was believed that the buffer plug was not necessary for the in-line derivatization.

As was discussed in the previous experiment, the next experiment would be to optimize the mixing voltage duration and ramp times to determine if the sensitivity could be improved even more.

Mixing voltage duration and ramp times

Since the mixing voltage was only meant to mix the FMOC and amino acid plug together it was believed this would also happen during the separation voltage. The only difference would be the amount of voltage used and thus the speed in which the plugs pass each other. This speed could also be influenced by adjusting the ramp time of the separation voltage. Therefore it was hypothesized that the mixing voltage was not necessary and could be replaced by adjusting the ramp time.

The CE method for in-line derivatization was used to enantioseparate the mixture with different ramp times. The runs were made with no mixing voltage and with a ramp time of 5 - 2 - 1 - 0.5 - 0.17 minutes.
The S/N ratios of L-Met, L-Phe and L-Asp were compared with each other to determine which ramp times obtained the best S/N ratios. The enantiomers L-Met, L-Phe and L-Asp were chosen for the comparison because they were relatively spread out in the migration window. Also, based on previous results in this study, these peaks often had good baseline separation which made the S/N ratio more accurate.

See Table 16 for the results.

Table 16: Overview of the obtained S/N ratios of L-Met, L-Phe and L-Asp from the in-line derivatized amino acid mixture with different ramp times in minutes

	L-MET			L-PHE			L-ASP		
Ramp time	Signal	Noise	S/N	Signal	Noise	S/N	Signal	Noise	S/N
0.17 minutes	580	1.6	363	1079	1.0	1079	374	1.2	312
0.5 minutes	751	1.7	442	1520	1.2	1267	513	1.2	428
1 minute	502	1.6	314	1180	1.5	787	578	1.2	482
2 minutes	1170	1.2	975	1523	0.8	1904	1003	1.1	912
5 minutes	971	1.4	694	1445	1.1	1314	950	1.2	792

All amino acids were successfully observed and enantioseparated in all runs.
The run with 2 minutes of ramp time had the best S/N ratio.

The run with a ramp time of 0.17 minutes used the same parameters as the run from Table 15 with no buffer time, except for the mixing voltage. But the S/N ratio's obtained in this experiment with the 0.17 ramp time was circa 2 to 3 times lower than the S/N ratio's obtained with the no buffer run from Table 15. This indicates that the exclusion of the mixing voltage did influence the sensitivity, and it was believed that the mixing voltage was necessary to improve the derivatization yield. The reason for this was because it was believed that the derivatization reaction needs a certain amount of time. With the mixing voltage of 3 kV for 72 seconds, the FMOC and amino acid plug pass each other slowly. So if the FMOC and the amino acid plug pass each other too quickly (due to the high separation voltage), there was not enough time for all the amino acids to be derivatized. Therefore it was believed that the run with a ramp time of 0.17 minutes had a lower derivatization yield compared to the no buffer run from Table 15, which explains the lower S/N ratios.

The idea of increasing the ramp time was to replace the function of the mixing voltage, to give the derivatization reaction enough time to derivatize most of the amino acids. The run with the 1 minute ramp time had S/N ratios which were lower compared to the S/N ratios of all other runs from Table 16. It was unknown why this happened, it might have been due to a faulty run.
The run with the 2 minutes ramp time had the highest S/N ratios compared to the other runs, and compared to that run a decrease in S/N ratios was observed for the run with 5 minutes ramp time. This decrease might have been due to diffusion of the amino acid peaks, and it was therefore believed that increasing the ramp time even more would only reduce the S/N ratios.

The run with 2 minutes ramp time had similar S/N ratios as the run with no buffer time from Table 15 (circa 7% difference). This indicates that no sensitivity was gained by removing the mixing voltage and increasing the ramp time. However it does indicate that the increased ramp time successfully replaced the mixing voltage. Using an increased ramp time was preferred over the mixing voltage because this effectively decreases the amount of steps needed to do a run.

It was concluded that a ramp time of 2 minutes gave the most optimal results compared to the results with the other ramp times.
Now that many parameters were changed, the potential amino acids Ala, Pro, Gln, Thr, Val and Leu need to be remeasured to determine if they could be added to the mixture.

Final method

With all the parameters optimized it was possible that more amino acids could be added to the mixture. The CE method for in-line derivatization was used to enantioseparate all the mixtures. First the amino acid mix of Met, Ile, Phe, Glu, Asp and Tyr was measured, this run was also used as a reference sample. If similar FMOC peaks were obtained with the other runs as with the reference run, the run was deemed successful. His, Arg, Asn, Ser, Cys, Lys, Ala, Pro, Gln and Thr were all individually measured, and Val and Leu were both separately mixed with the amino acid mixture and measured.
The resolution and LOD was determined for the enantiomers of Tyr, Met, Ile, Phe, Glu and Asp from the amino acid mixture.

See Figure 26 and Table 17 for the results.

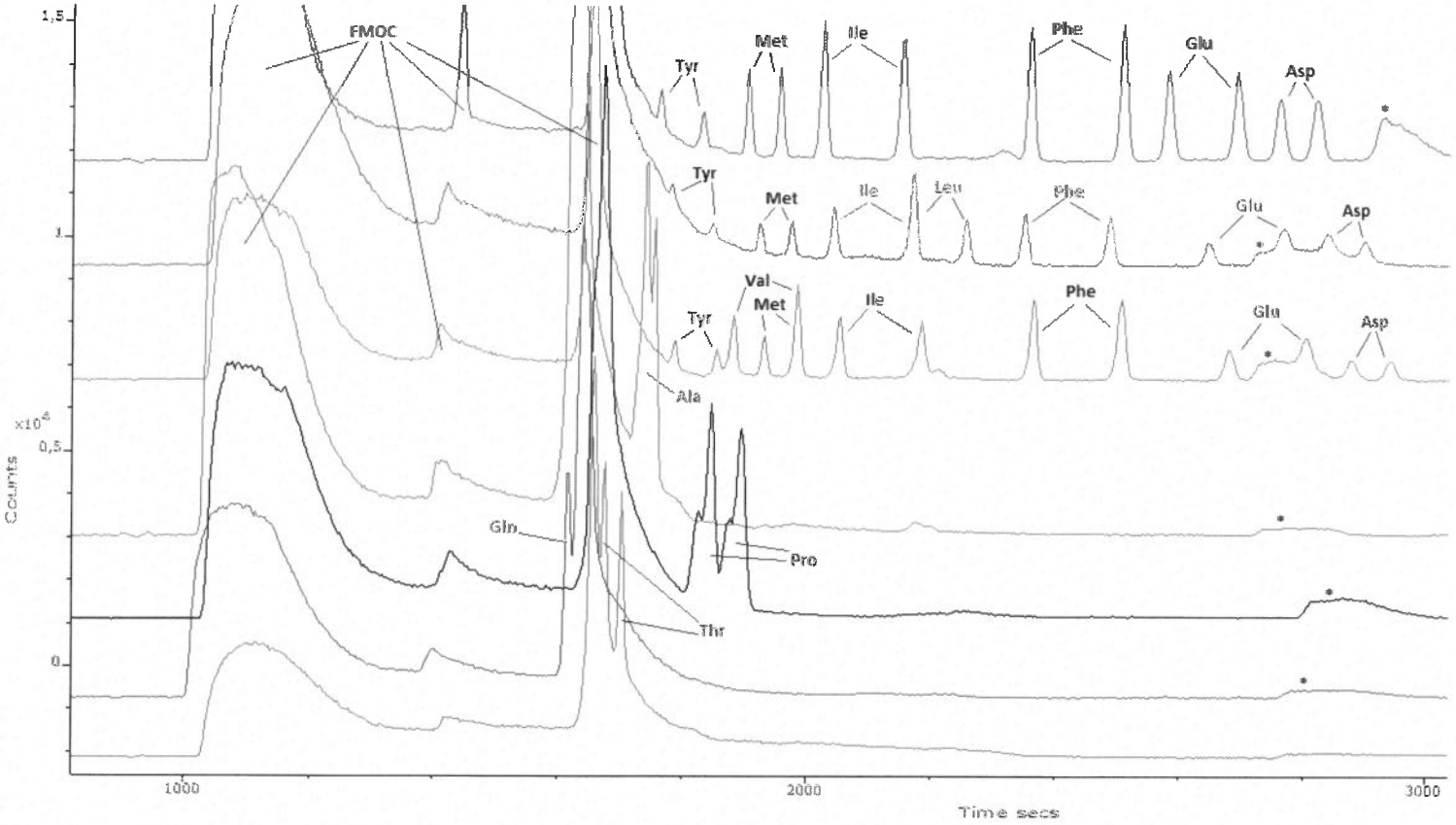

Figure 26: Electropherograms of the in-line derivatized mixture of |Met, Ile, Phe, Glu, Asp & Tyr|, Met, Ile, Phe, Glu, Asp, Tyr & Leu|, Met, Ile, Phe, Glu, Asp, Tyr & Val|, the individual measured amino acids Ala, Pro, Gln and Thr from top to bottom respectively.
All runs had the same FMOC peaks but not all those peaks were marked to maintain visibility.
Peaks marked with a * were impurities

Table 17: Overview of the obtained S/N ratios, R_s and LOD of all the enantiomers of Tyr, Met, Ile, Phe, Glu and Asp from the in-line derivatized amino acid mixture

Peak	R_s	S/N	LOD (nM)
D-Tyr	1.6	204	612
L-Tyr	3.4	203	615
D-Met	3.2	1066	117
L-Met	2.1	1043	120
D-Ile	2.6	1917	65
L-Ile	4.1	1683	74
D-Phe	6.4	1908	66
L-Phe	4.7	1913	65
D-Glu	2.1	1081	116
L-Glu	3.1	1041	120
D-Asp	1.9	867	144
L-Asp	1.6	875	143

The reference run with the amino acid mixture in Figure 26 was as expected. All other runs in Figure 26 were deemed successful because they had similar FMOC peaks as the reference run. Both enantiomers were observed for Ala, Pro and Thr, but there was no baseline separation between the enantiomers. Gln and Thr were both partially overlapping with the FMOC peak. Peaks marked with an * were impurities.

The results for Val and Leu in Figure 26 were very similar to the results from Figure 20, in both figures L-Val overlapped with L-Met and L-Leu overlapped with D-Ile.
His, Arg, Asn, Ser, Cys and Lys were not observed after 90 minutes.
All R_s values are >1,5 which means all enantiomers are baseline separated from each other.

There were no visually differences observed between Figure 26 and the results from Figure 20. In these results Val and Leu overlap with the same enantiomer, Ala and Pro have no baseline separation and Gln and Thr partially overlap with the FMOC peak. This would mean that no extra amino acids can be added to the current amino acid mixture while maintaining enantioseparation of all amino acids without any overlap.

This also means that the FMOC peak width reduction did not enable the addition of another amino acid to the mixture to successfully enantioseparate without overlap.

All R_s values are >1.5 which is better than the previously obtained R_s values in Table 12 which had 2 enantiomers with an R_s value of 1.4.
The LOD of the enantiomers of Tyr are circa 3 times higher compared to the LOD of the other enantiomers. This difference was most likely caused due to the fact that Tyr partially overlaps with the FMOC peak which increases the noise.

5.4 Validation

For the validation of the method the repeatability and the linearity were determined.

Repeatability

To determine the repeatability of the method the CE method for in-line derivatization was used to enantioseparate the amino acid mixture six times. The amino acid mixture was also off-line derivatized and measured 6 times to compare the off-line method with the in-line method. The difference between those results could determine the influence of the in-line derivatization procedure on the repeatability. From those 6 runs, one outlier was removed per enantiomer.

See Table 18, Table 19 and Table 20 for the results. See appendix 8.1 for the raw data.

Table 18: Overview of the obtained repeatability results from the in-line derivatized amino acid mixture based on 5 runs

	Corrected Area				Mobility		
	Average	STD	%STD		Average	STD	%STD
D-TYR	1,34	0,28	20,72	D-TYR	-8,56E-09	5,25E-11	0,61
L-TYR	1,46	0,24	16,30	L-TYR	-8,91E-09	5,61E-11	0,63
D-MET	3,68	0,33	8,95	D-MET	-9,27E-09	5,50E-11	0,59
L-MET	3,82	0,25	6,43	L-MET	-9,50E-09	5,40E-11	0,57
D-ILE	5,77	0,22	3,74	D-ILE	-9,80E-09	5,92E-11	0,60
L-ILE	5,14	0,49	9,44	L-ILE	-1,03E-08	5,88E-11	0,57
D-PHE	6,61	0,42	6,33	D-PHE	-1,09E-08	6,04E-11	0,55
L-PHE	6,69	0,32	4,73	L-PHE	-1,13E-08	5,82E-11	0,51
D-GLU	5,88	0,36	6,17	D-GLU	-1,17E-08	7,20E-11	0,62
L-GLU	5,45	0,23	4,26	L-GLU	-1,19E-08	7,25E-11	0,61
D-ASP	4,99	0,17	3,34	D-ASP	-1,21E-08	7,34E-11	0,61
L-ASP	4,49	0,58	12,94	L-ASP	-1,22E-08	7,28E-11	0,60

Table 19: Overview of the obtained repeatability results from the off-line derivatized amino acid mixture based on 5 runs

	Corrected Area		
	Average	STD	%STD
D-TYR	-	-	-
L-TYR	-	-	-
D-MET	2,02	0,15	7,41
L-MET	2,01	0,13	6,49
D-ILE	2,55	0,25	9,63
L-ILE	2,15	0,11	4,95
D-PHE	3,00	0,18	6,09
L-PHE	3,12	0,12	3,98
D-GLU	5,88	0,22	3,74
L-GLU	6,02	0,25	4,14
D-ASP	6,33	0,26	4,05
L-ASP	6,36	0,23	3,58

Table 20: Overview of the F-test results between the off-line and in-line measurements

Corrected Area			
	F_{cal}		F(0.005, 4, 4)
D-MET	4.81	<	9.60
L-MET	3.56	<	9.60
D-ILE	1.29	<	9.60
L-ILE	20.7	>	9.60
D-PHE	5.23	<	9.60
L-PHE	6.47	<	9.60
D-GLU	2.72	<	9.60
L-GLU	1.15	<	9.60
D-ASP	2.36	<	9.60
L-ASP	6.50	<	9.60

The relative standard deviation of the corrected area of Tyr was higher when compared to the other amino acids for both the off- and in-line results. For the rest of the amino acids the relative standard deviation was more or less <7%. Tyr could not be observed with the off-line derivatized runs. The relative standard deviation for the corrected area for the rest of the amino acids was average <6%. The relative standard deviation for the mobility of the in-line derivatized amino acid mixture was <0.63%.

The high %STD of Tyr was most likely due to the partial overlap with the FMOC peak. This overlap of Tyr with the FMOC peak was not always observed, recent results have shown Tyr with and without overlap as can been seen in Figure 26. Tyr was not observed with off-line derivatization, this also happened in the past with Tyr. It was believed that the reason for this was because the Tyr was not completely dissolved in the solution, with which the off-line derivatization was performed.

It was visually observed that the off-line derivatized measurements have a relatively lower average and %STD compared to the in-line measurements.
To determine if the standard deviations between the off-line and in-line derivatized measurements were significantly different the F-test was used. As seen in the results in Table 20 the standard deviations between de off-line and in-line measurements are not significantly different, except for L-Ile. It was unknown why only L-Ile had a significantly different standard deviation. This indicated that the in-line derivatization procedure had no significant influence on the standard deviation of the results, except for L-Ile.
To determine if the averages of the off-line and in-line derivatized measurements were significantly different from each other the paired t-test was used.
$T_{cal} = 63.2$
$T(0.05, 49) = 2.01$
$T_{cal} > T = 63.2 > 2.01$
This meant that the averages of the off-line and in-line derivatized measurements were significantly different from each other. This indicated that the in-line derivatization procedure had a significant influence on the average corrected area even though the standard deviation of the results were not significantly different (except for L-Ile).

After consultation it was believed that a %STD of the corrected area of 3 - 9% was acceptable enough for this kind of method.
The %STD for the mobility was for all enantiomers in a range of 0.5 - 0.6%. This indicated that the mobility of the enantiomers barely shift.

Linearity

To determine the linearity of the method the CE method for in-line derivatization was used to enantioseparate the amino acid mixture with different amino acid concentrations. A high and a low range concentration was measured. The high range consisted of 41.7 - 33.3 - 25 - 16.7 - 8.3 μM concentration per enantiomer (500 to 100 μM total concentration), and the low range consisted of 10.4 - 8.3 - 6.3 - 4.2 - 2.1 μM concentration per enantiomer (125 to 25 μM total concentration).

See Table 21, Figure 27 and Figure 28 for the results. See appendix 8.2 for the raw data and all other figures.

Table 21: Overview of the obtained R^2 values of the linearity results from the in-line derivatized amino acid mixture with both high and low end amino acid concentrations.

	R^2 (area)	
	High end (41.7 - 8.3 μM)	Low end (10.4 - 2.1 μM)
D-TYR	0.9830	-
L-TYR	0.9846	-
D-MET	0.9877	0.9806
L-MET	0.9927	0.9837
D-ILE	0.9956	0.991
L-ILE	0.9976	0.9927
D-PHE	0.9946	0.997
L-PHE	0.9938	0.9902
D-GLU	0.9811	0.9921
L-GLU	0.9801	0.9917
D-ASP	0.9805	0.9916
L-ASP	0.9817	0.9804

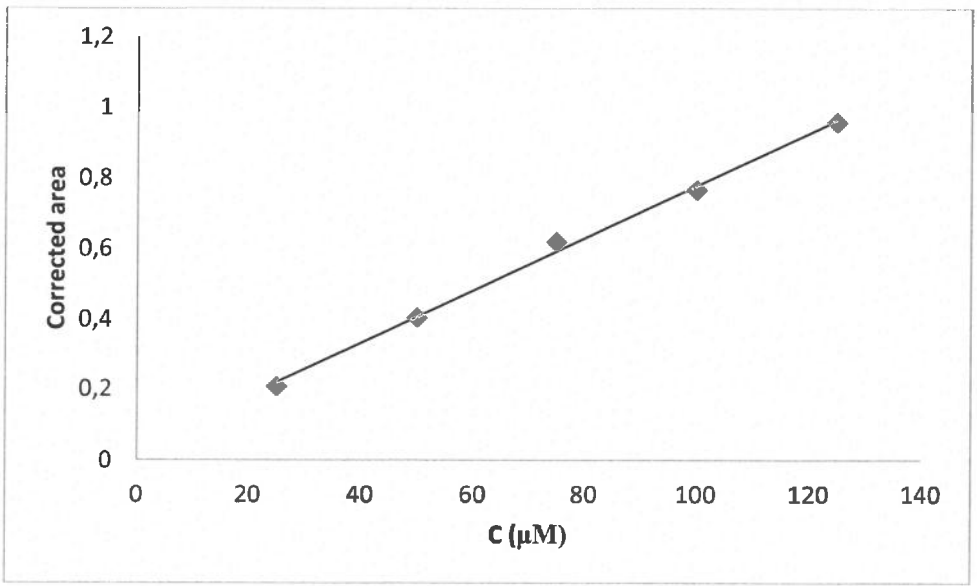

Figure 27: Calibration curve of D-Phe low end, with the corrected areas on the y-axis and the concentration on the x-axis. y=0.03(+/0.11)+0.0077(+/-0.0017)x ; sy/x = 0.0218 n = 5 ; R2 = 0,9970 ; 95%

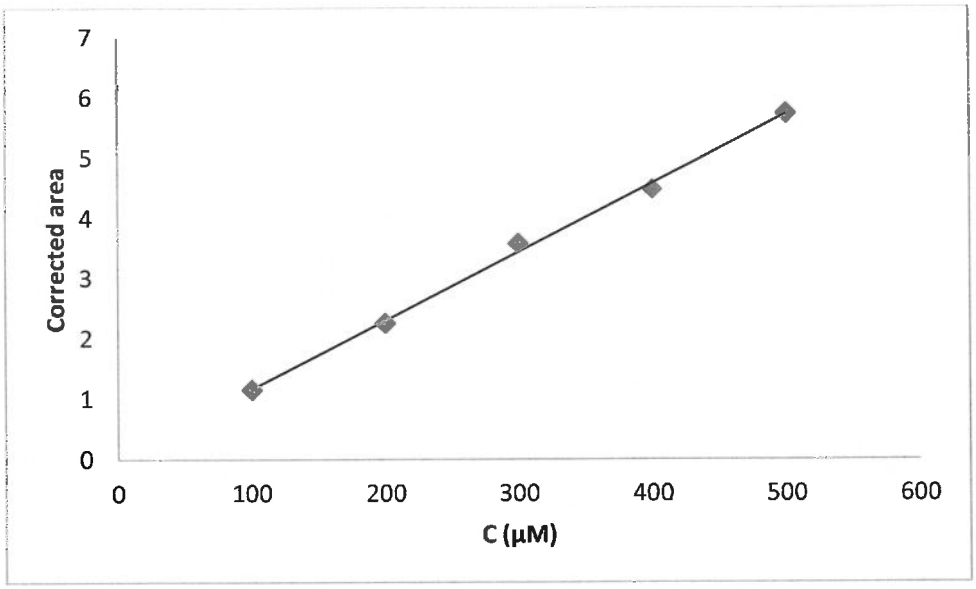

Figure 28: Calibration curve of D-Phe high end, with the measured areas on the y-axis and the concentration on the x-axis. y=-0.0(+/1.0)+0.0114(+/-0.0036)x ; sy/x = 0.1876; n = 5 ; R2 = 0,9946 ; 95%

Based on the peak area all enantiomers had a R^2 of 0.98 or higher in both the high and low end of concentrations except for Tyr, of which the enantiomers were not observed at the 4.2 and 2.1 µM concentration.

Based on the graphs in Figure 27 and Figure 28 of D-Phe from both the low and high end (see appendix 8.2 for the rest of the figures) and Table 21 it was believed that all the enantiomers were linear in both the high and low end, except for Tyr. This was because the Tyr enantiomers were not observed with the lowest concentrations, 4.2 and 2.1 µM, because the peak was too small to be observed. Bases on the calculated LOD of circa 600 nm for Tyr in Table 17 it was expected Tyr could be observed. It might be possible that due to the low concentration of Tyr the derivatization yield was less compared to the higher concentrations used for the results in Table 17.
For Tyr the linear range was 41.7 to 8.3 µM. For all other amino acids the range was 41.7 to 2.1 µM.

5.5 Real sample

The next step was to measure a biological sample. If the amino acids could be observed in urine for example, it might be possible to develop a quantitative method based on the current method.

The CE method for in-line derivatization was used to enantioseparate a urine sample spiked with the amino acid mixture. The sample was prepared by taking 1500µl urine, add 100µl of 1 M NaOH, 200µl water and 200µl of the amino acid mixture. The pH of this sample was 9.4, the same as the tetraborate buffer used for BGE.
The amino acid mixture was added to make sure that the concentration of the amino acids in the sample was high enough to be measured with the method to test the feasibility of enantioseparation in this mixture.

See Figure 29 for the results.

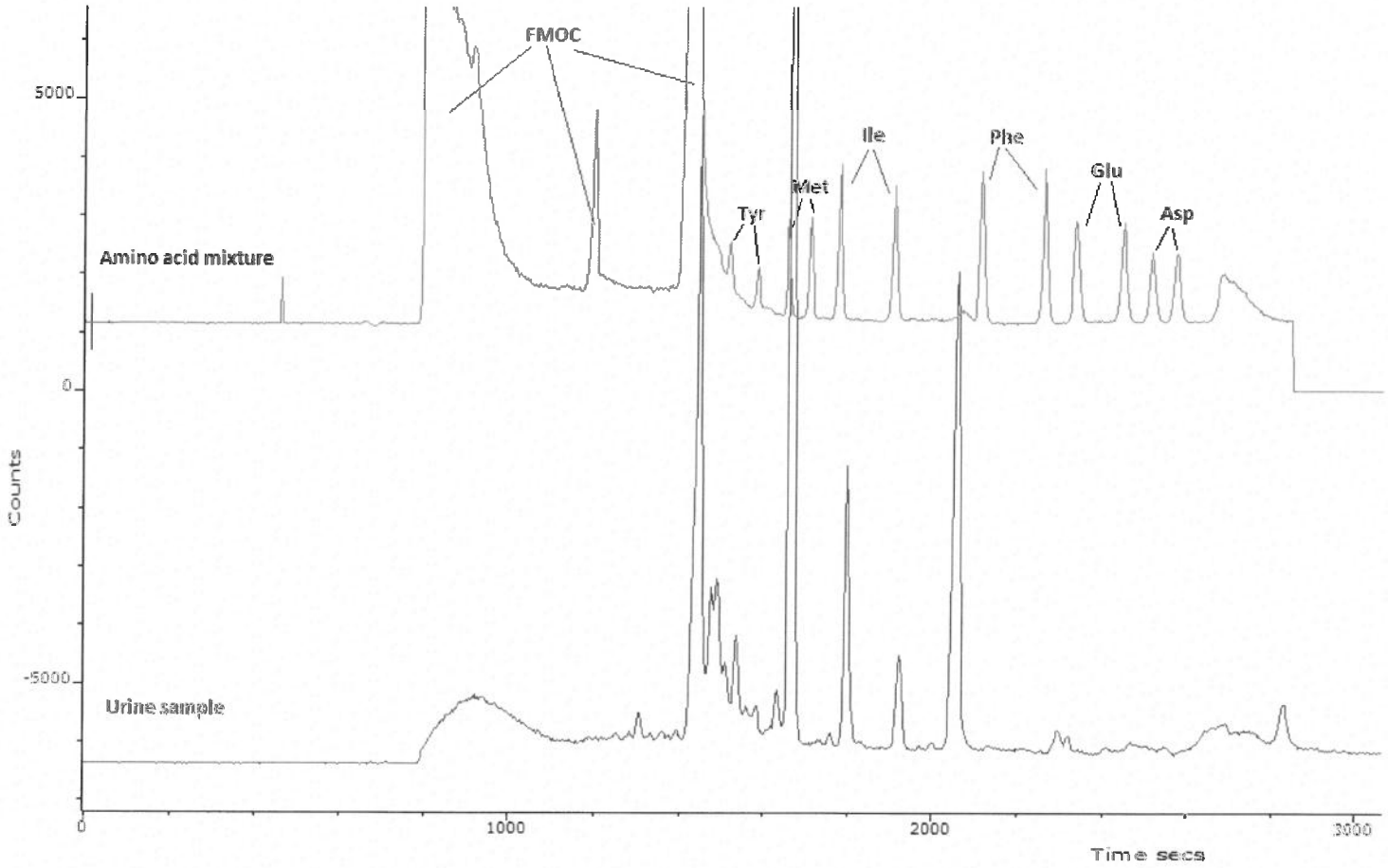

Figure 29: Electropherograms of the in-line derivatized urine sample spiked with the amino acid mixture and the amino acid mixture itself for comparison. The amino acid mixture consists of Tyr, Met, Ile, Phe, Glu and Asp.

The electropherogram of the amino acid mixture was the same one from Figure 26, it was added for comparison.

It was observed that the FMOC peaks from the urine sample had lower signal intensities compared to the FMOC peaks from the amino acid mixture. Multiple peaks were observed from the urine sample, but it was unknown where the peaks originated from.

Because the FMOC peaks from the urine sample were a lot smaller it was believed that the FMOC also reacted with other components in the urine besides the amino acids. Because urine is a complex matrix (containing a wide variety of metabolites, hormones and proteins) it was believed that the FMOC reacted with other components besides the amino acids. This could also explain why many of the amino acid peaks were not observed, because most of the FMOC reacted with other components in the urine sample which resulted in a low derivatization yield of the amino acids.

There were multiple peaks observed from the urine sample, but it was unknown where the peaks originated from. It might be possible that some of those peaks originated from the amino acids but it was believed that many of those peaks were the result of the reaction of the FMOC with the urine matrix. This could be verified by spiking the urine sample with one of the enantiomers, and repeat this for every enantiomer. When spiked with one enantiomer and a strong increase in signal intensity would be observed in one peak, it would be most likely that that peak originated from the spiked enantiomer.

6 Conclusion

The goal of this study was to develop an efficient and sensitive method to chirally separate amino acids using in-line derivatization with 9-fluoroenylmethyl chloroformate. β-cyclodextrin was used as a chiral selector combined with micellar electrokinetic chromatography. The background electrolyte consisted of 40 mM sodium tetraborate, pH 9.4, 25 mM sodium dodecyl sulfate, 17% isopropanol and 30 mM β-cyclodextrin. Fluorescence detection was used for sensitive detection.

A method has been developed with which it is possible to successfully enantioseparate 6 amino acids in one sample, tyrosine, methionine, isoleucine, phenylalanine, glutamic acid and aspartic acid. The 6 aforementioned amino acids and its individual enantiomers can be detected in a linear range from 41.7 to 2.1 µM with 3 - 9 %STD. Except for tyrosine, which can be detected in a linear range from 41.7 to 8.3 µM. Valine, leucine, glycine, proline, alanine and tryptophan can also be detected and enantioseparated with this method but they overlap with other amino acids when they are added to the other 6. With this method the D-enantiomer elutes before the L-enantiomer with all observed

The parameters for the optimized method are shown in Table 22, the in-line derivatization was performed by first injecting the amino acid sample followed by the injection of the FMOC solution.

Table 22: Parameters for the optimized in-line derivatization method with FMOC and fluorescence detection

Parameters	
Capillary	75 µm ID, 79 cm total length (65 cm to window)
Detector	Fluorescence (emission at 330±10 nm)
Temperature	25 °C
Voltage	30 kV (2 minutes ramp time)
Amino acid injection	10 seconds (0.3 psi)
FMOC injection	8 seconds (0.3 psi)
FMOC concentration	10 mM
BGE	
Concentration sodium tetraborate	40 mM
Concentration iso-propanol	17%
Concentration SDS	25 mM
Concentration β-CD	30 mM

The next step for this study would be complex matrices. Not many experiments were performed on urine samples during this study, and no amino acid peaks were identified. A lot of unidentified peaks were observed, and therefore a good next step would be to determine where those peaks originate from. This could be done by spiking the urine sample with a high concentration of a single enantiomer.
A different biological could also be explored, for example cerebrospinal fluid.
It is also recommended to explore the effects of adding different cyclodextrins to the BGE, for example γ-CD. It might be possible that the by adding different cyclodextrins, the migration order of the amino acids change, which could result in the possibility to add more amino acids to the mixture.

7 References

1. Friedman M., Levin C.E.,
Nutritional and medicinal aspects of D-amino acids,
2012, Amino Acids, 42, 1553-1582.

2. Kenji Hamase, Akiko Morikawa, Kiyoshi Zaitsu,
d-Amino acids in mammals and their diagnostic value,
Journal of Chromatography B, Volume 781, Issues 1–2, 5 December 2002, Pages 73–91.

3. Hiroko Ohide, Yurika Miyoshi, Rindo Maruyama, Kenji Hamase, Ryuichi Konno,
d-Amino acid metabolism in mammals: Biosynthesis, degradation and analytical aspects of the metabolic study,
Journal of Chromatography B, Volume 879, Issue 29, 1 November 2011, Pages 3162-3168.

4. Sabine A. Fuchs, Ruud Berger, Leo W.J. Klomp, Tom J. de Koning,
d-Amino acids in the central nervous system in health and disease,
Molecular Genetics and Metabolism, Volume 85, Issue 3, July 2005, Pages 168-180.

5. Hashimoto A., Kumashiro S., Nishikawa T., Oka T., Takahashi K., Mito T., Takashima S., Doi N., Mizutani Y., Yamazaki T.,
Embryonic development and postnatal changes in free D-aspartate and D-serine in the human prefrontal cortex,
Journal of Neurochemistry, July 1993, 61(1):348 - 351.

6. George H. Fisher, Antimo D'Aniello, Amedeo Vetere, Lucia Padula, Gregory P. Cusano, Eugene H. Man,
Free D-aspartate and D-alanine in normal and Alzheimer brain,
Brain Research Bulletin, Volume 26, Issue 6, June 1991, Pages 983–985.

7. Hans Brückner, Michael Hausch,
Gas chromatographic characterization of free d-amino acids in the blood serum of patients with renal disorders and of healthy volunteers,
Journal of Chromatography B: Biomedical Sciences and Applications, Volume 614, Issue 1, 21 April 1993, Pages 7–17.

8. Fradi I., Servais A.C., Lamalle C., Kallel M., Abidi M., Crommen J., Fillet M.,
Chemo- and enantio-selective method for the analysis of amino acids by capillary electrophoresis with in-capillary derivatization,
Journal of Chromatography A, 1267 (2012) 121-126.

9. Fradi I., Farcas E., Saïd A.B., Yans M.L., Lamalle C., Somsen G.W., Prior A., de Jong G.J., Kallel M., Crommen J., Servais A.C., Fillet M.,
In-capillary derivatization with (−)-1-(9-fluorenyl)ethylchloroformate as chiral labeling agent for the electrophoreticseparation of amino acids,
Journal of Chromatography A, Volume 1363, 10 October 2014, Pages 338–347.

10. Hong Wan, Lars G. Blomberg,
Chiral separation of amino acids and peptides by capillary electrophoresis,
Journal of Chromatography A, Volume 875, Issues 1–2, 14 April 2000, Pages 43-88.

11. F.E.P. Mikkers, F.M. Everaerts, Th.P.E.M. Verheggen,
High-performance zone electrophoresis,
Journal of Chromatography A, Volume 169, 1 February 1979, Pages 11–20.

12. J.W. Jorgenson, K.D. Lukacs,
Zone Electrophoresis in Open-Tubular Glass Capillaries,
Analytical Chemistry, 53, 1298-1302 (1981).

13. Stellan Hjertén,
High-performance electrophoresis: the electrophoretic counterpart of high-performance liquid chromatography,
Journal of Chromatography A, Volume 270, 1983, Pages 1-6.

14. Koji Otsuka, Shigeru Terabe,
Enantiomeric separation by micellar electrokinetic chromatography,
TrAC Trends in Analytical Chemistry, Volume 12, Issue 4, April 1993, Pages 125-130.

15. Primer A.,
High Performance Capillary Electrophoresis,
Germany, second completely revised edition, PN: 5990-3777EN.

16. De Kort, B.J., de Jong, G.J., Somsen, G.W.,
Native fluorescence detection of biomolecular and pharmaceutical compounds in capillary electrophoresis: detector designs, performance and applications: a review,
Analytica Chimica Acta, Volume 766, 5 March 2013, Pages 13–33.

17. De Kort, B.J., de Jong, G.J., Somsen, G.W.,
Lamp-based wavelength-resolved fluorescence detection for protein capillary electrophoresis: Setup and detector performance,
Electrophoresis, Volume 31, Issue 17, pages 2861–2868, September 2010.

18. Li Qi, Gengliang Yang,
On-column labeling technique and chiral ligand-exchange CE with zinc(II)-L-arginine complex as a chiral selector for assay of dansylated D,L-amino acids,
Electrophoresis, Volume 30, Issue 16, pages 2882–2889, August 2009.

19. Maria Teresa Veledo, Mercedes de Frutos, Jose Carlos Diez-Masa,
Amino acids determination using capillary electrophoresis with on-capillary derivatization and laser-induced fluorescence detection,
Journal of Chromatography A, Volume 1079, Issues 1–2, 24 June 2005, Pages 335–343.

20. A.B. Martínez-Girón, C. García-Ruiz , A.L. Crego, M.L. Marina,
Development of an in-capillary derivatization method by CE for the determination of chiral amino acids in dietary supplements and wines,
Electrophoresis, Volume 30, Issue 4, pages 696–704, February 2009.

21. Luc Denoroy, Sandrine Parrot, Louis Renaud, Bernard Renauda, Luc Zimmer,
In-capillary derivatization and capillary electrophoresis separation of amino acid neurotransmitters from brain microdialysis samples,
Journal of Chromatography A, Volume 1205, Issues 1–2, 26 September 2008, Pages 144–149.

22. Adam S. Ptolemy, Lara Tran, Philip Britz-McKibbin,
Single-step enantioselective amino acid flux analysis by capillary electrophoresis using on-line sample preconcentration with chemical derivatization,
Analytical Biochemistry, Volume 354, Issue 2, 15 July 2006, Pages 192–204.

23. Rosa M Latorre, Santiago Hernández-Cassou, Javier Saurina,
Strategies for in-capillary derivatization of amino acids in capillary electrophoresis using 1,2-naphthoquinone-4-sulfonate as a labeling reagent,
Journal of Chromatography A, Volume 934, Issues 1–2, 16 November 2001, Pages 105–112.

24. Yanli Han, Yi Chen,
On-column labeling technique and chiral CE of amino acids with mixed chiral selectors and UV detection,
Electrophoresis, Volume 28, Issue 15, pages 2765–2770, No. 15 August 2007.

25. Hong Wan, Per E. Andersson, Anders Engström, Lars G. Blomberg,
Direct and indirect chiral separation of amino acids by capillary electrophoresis,
Journal of Chromatography A, Volume 704, Issue 1, 2 June 1995, Pages 179–193.

26. E.M.Martin Del Valle,
Cyclodextrins and their uses: a review,
Process Biochemistry, Volume 39, Issue 9, 31 May 2004, Pages 1033–1046.

27. Gabriel Hancu, Aura Rusu, Brigitta Simon, Georgiana Boia, Árpád Gyéresi,
Simultaneous separation of ciprofloxacin, norfloxacin and ofloxacin by micellar electrokinetic chromatography,
J. Braz. Chem. Soc. vol.23 no.10 São Paulo Oct. 2012 Epub Oct 26, 2012.

28. Patrick Shahgaldian, Uwe Pieles,
Cyclodextrin Derivatives as Chiral Supramolecular Receptors for Enantioselective Sensing,
Sensors (Basel). 2006 Jun; 6(6): 593–615.

8 Raw data

8.1 Repeatability

Injection of Amino acid mix of 500 uM total concentration (41,67 uM of each enantiomer), repeated 6 times

	Filename		Migration time	Area	C. Area	mean	STD	%STD
D-TYR	150513 01	1	30,6	4609	1,631727	1,472359	0,408098	27,7173
	150513 02	2	29,95	4437	1,604925			
	150513 03	3	29,6	3186	1,166047			
	150513 04	4	28,9	3486	1,306747			
	150513 05	5	29,65	2713	0,991259			
	150513 06	6	29,35	5780	2,133447			
			Migration time	Area	C. Area	mean	STD	%STD
L-TYR		1	31,75	6249	2,132205	1,569083	0,348135	22,1872
		2	31,1	5184	1,805788			
		3	30,75	4197	1,478618			
		4	30,05	3669	1,322712			
		5	30,75	4275	1,506098			
		6	30,45	3286	1,169075			
			Migration time	Area	C. Area	mean	STD	%STD
D-MET		1	33,05	11879	3,893772	3,59739	0,352058	9,786488
		2	32,35	12011	4,022231			
		3	32	9776	3,309583			
		4	31,25	9637	3,340827			
		5	32,05	11286	3,814821			
		6	31,65	9358	3,203107			
			Migration time	Area	C. Area	mean	STD	%STD
L-MET		1	33,95	11986	3,824374	3,735477	0,306483	8,204643
		2	33,2	12749	4,160065			
		3	32,85	10738	3,541197			
		4	32,1	10787	3,640472			
		5	32,9	11987	3,947087			
		6	32,5	9899	3,299667			
			Migration time	Area	C. Area	mean	STD	%STD
D-ILE		1	35,15	18275	5,632409	5,586533	0,49512	8,862748
		2	34,4	19492	6,138469			
		3	34,05	18078	5,751689			
		4	33,3	17192	5,592993			
		5	34,05	18065	5,747553			
		6	33,7	14484	4,656083			
			Migration time	Area	C. Area	mean	STD	%STD
L-ILE		1	37,45	16930	4,897419	5,382732	0,737451	13,70032
		2	36,6	19320	5,718579			
		3	36,15	22023	6,599793			
		4	35,4	16508	5,051883			
		5	36,2	18441	5,518715			
		6	35,75	14863	4,51			

	1 point removed			migration time		
	mean	STD	%STD	mean	STD	%STD
D-TYR	1,340141	0,277613	20,71518	29,675	0,573367	1,932156
L-TYR	1,456458	0,237415	16,30084	30,80833	0,580014	1,882654
D-MET	3,676247	0,32908	8,951511	32,05833	0,615156	1,918864
L-MET	3,822639	0,245836	6,431048	32,91667	0,631401	1,918179
D-ILE	5,772622	0,216123	3,743935	34,10833	0,631994	1,852903
L-ILE	5,139319	0,485203	9,440994	36,25833	0,713734	1,96847

mobility

	apparent mobility	EOF time	mobility EOF	mobility	1 point removed mean	STD	%STD
D-TYR	9,3228E-09	16	1,78299E-08	-8,50706E-09	-8,5603E-09	5,24674E-11	0,612915
	9,52513E-09	15,7	1,81706E-08	-8,64542E-09			
	9,63776E-09	15,7	1,81706E-08	-8,5328E-09			
	9,8712E-09	14,9	1,91462E-08	-9,27496E-09			
	9,62151E-09	15,7	1,81706E-08	-8,54905E-09			
	9,71986E-09	15,6	1,8287E-08	-8,56718E-09			
L-TYR	8,98513E-09	16	1,78299E-08	-8,84473E-09	-8,9094E-09	5,60582E-11	0,629201
	9,17292E-09	15,7	1,81706E-08	-8,99764E-09			
	9,27733E-09	15,7	1,81706E-08	-8,89323E-09			
	9,49344E-09	14,9	1,91462E-08	-9,65272E-09			
	9,27733E-09	15,7	1,81706E-08	-8,89323E-09			
	9,36873E-09	15,6	1,8287E-08	-8,91831E-09			
D-MET	8,6317E-09	16	1,78299E-08	-9,19816E-09	-9,2698E-09	5,50395E-11	0,593752
	8,81848E-09	15,7	1,81706E-08	-9,35208E-09			
	8,91493E-09	15,7	1,81706E-08	-9,25563E-09			
	9,12889E-09	14,9	1,91462E-08	-1,00173E-08			
	8,90102E-09	15,7	1,81706E-08	-9,26954E-09			
	9,01352E-09	15,6	1,8287E-08	-9,27352E-09			
L-MET	8,40288E-09	16	1,78299E-08	-9,42698E-09	-9,5E-09	5,40063E-11	0,568438
	8,5927E-09	15,7	1,81706E-08	-9,57785E-09			
	8,68426E-09	15,7	1,81706E-08	-9,4863E-09			
	8,88716E-09	14,9	1,91462E-08	-1,0259E-08			
	8,67106E-09	15,7	1,81706E-08	-9,4995E-09			
	8,77778E-09	15,6	1,8287E-08	-9,50926E-09			
D-ILE	8,11601E-09	16	1,78299E-08	-9,71385E-09	-9,7996E-09	5,92363E-11	0,604477
	8,29296E-09	15,7	1,81706E-08	-9,8776E-09			
	8,3782E-09	15,7	1,81706E-08	-9,79236E-09			
	8,5669E-09	14,9	1,91462E-08	-1,05793E-08			
	8,3782E-09	15,7	1,81706E-08	-9,79236E-09			
	8,46522E-09	15,6	1,8287E-08	-9,82182E-09			
L-ILE	7,61756E-09	16	1,78299E-08	-1,02123E-08	-1,0293E-08	5,87842E-11	0,571113
	7,79447E-09	15,7	1,81706E-08	-1,03761E-08			
	7,8915E-09	15,7	1,81706E-08	-1,02791E-08			
	8,05869E-09	14,9	1,91462E-08	-1,10875E-08			
	7,8806E-09	15,7	1,81706E-08	-1,029E-08			
	7,9798E-09	15,6	1,8287E-08	-1,03072E-08			

1 point removed

migration time

1 point removed

		Migration time	Area	C. Area	mean	STD	%STD
D-PHE	1	40,75	24210	6,436196	6,888791	0,808206	11,68619
	2	39,75	30663	8,356792			
	3	39,25	24940	6,856051			
	4	38,45	23117	6,513242			
	5	39,3	25983	7,162405			
	6	38,85	21761	6,068061			

1 point removed			
mean	STD	%STD	
6,807191	0,418007	6,32655	

migration time			
mean	STD	%STD	
39,39167	0,797757	2,025193	

apparent mobility	EOF time	mobility EOF	mobility
7,00068E-09	16	1,78299E-08	-1,08292E-08
7,17698E-09	15,7	1,81706E-08	-1,09938E-08
7,26822E-09	15,7	1,81706E-08	-1,09023E-08
7,41945E-09	14,9	1,91462E-08	-1,17267E-08
7,25898E-09	15,7	1,81706E-08	-1,09116E-08
7,34306E-09	15,6	1,8287E-08	-1,0944E-08

1 point removed			
mean	STD	%STD	
-1,0916E-08	8,038E-11	0,552942	

		Migration time	Area	C. Area	mean	STD	%STD
L-PHE	1	43,25	26648	6,674836	6,989563	0,792931	11,3445
	2	42,05	33000	8,501784			
	3	41,5	25950	6,774096			
	4	40,75	25290	6,723313			
	5	41,6	27149	7,070052			
	6	41,15	23525	6,193297			

1 point removed			
mean	STD	%STD	
6,887119	0,31604	4,726094	

migration time			
mean	STD	%STD	
41,71667	0,869291	2,083798	

apparent mobility	EOF time	mobility EOF	mobility
6,59602E-09	16	1,78299E-08	-1,12338E-08
6,76425E-09	15,7	1,81706E-08	-1,13863E-08
6,87416E-09	15,7	1,81706E-08	-1,12964E-08
7,00068E-09	14,9	1,91462E-08	-1,21455E-08
6,85764E-09	15,7	1,81706E-08	-1,13129E-08
6,93263E-09	15,6	1,8287E-08	-1,13544E-08

1 point removed			
mean	STD	%STD	
-1,1317E-08	5,92209E-11	0,514466	

		Migration time	Area	C. Area	mean	STD	%STD
D-GLU	1	45,5	22698	5,404286	6,034642	0,506024	8,385317
	2	44,5	26360	6,417228			
	3	43,75	23939	5,927752			
	4	43,1	23187	5,826132			
	5	43,75	27573	6,9276			
	6	43,2	23140	5,802855			

1 point removed			
mean	STD	%STD	
5,876051	0,362547	6,169916	

migration time			
mean	STD	%STD	
43,96667	0,902035	2,051633	

apparent mobility	EOF time	mobility EOF	mobility
6,26984E-09	16	1,78299E-08	-1,156E-08
6,41074E-09	15,7	1,81706E-08	-1,17598E-08
6,52063E-09	15,7	1,81706E-08	-1,16499E-08
6,61897E-09	14,9	1,91462E-08	-1,25272E-08
6,52063E-09	15,7	1,81706E-08	-1,16499E-08
6,60365E-09	15,6	1,8287E-08	-1,16834E-08

1 point removed			
mean	STD	%STD	
-1,1681E-08	7,19524E-11	0,617055	

		Migration time	Area	C. Area	mean	STD	%STD
L-GLU	1	47,55	22290	5,078339	5,66964	0,578042	10,21302
	2	46,45	23802	5,551238			
	3	45,6	23763	5,64545			
	4	45	22308	5,370444			
	5	45,85	28541	6,773147			
	6	45,1	23310	5,599224			

1 point removed			
mean	STD	%STD	
5,448939	0,231934	4,256494	

migration time			
mean	STD	%STD	
45,89167	0,961986	2,09621	

apparent mobility	EOF time	mobility EOF	mobility
5,99953E-09	16	1,78299E-08	-1,18303E-08
6,14161E-09	15,7	1,81706E-08	-1,20289E-08
6,25609E-09	15,7	1,81706E-08	-1,19145E-08
6,33951E-09	14,9	1,91462E-08	-1,28067E-08
6,24924E-09	15,7	1,81706E-08	-1,19213E-08
6,32545E-09	15,6	1,8287E-08	-1,19616E-08

1 point removed			
mean	STD	%STD	
-1,1931E-08	7,25102E-11	0,607729	

		Migration time	Area	C. Area	mean	STD	%STD
D-ASP	1	48,8	23112	5,130738	4,746645	0,618397	13,02808
	2	47,85	21663	4,925131			
	3	46,9	20440	4,731481			
	4	46,2	21543	5,051569			
	5	46,95	22139	5,119239			
	6	46,3	15051	3,521652			

1 point removed			
mean	STD	%STD	
4,991644	0,16694	3,342387	

migration time			
mean	STD	%STD	
47,1	0,979285	2,079162	

apparent mobility	EOF time	mobility EOF	mobility
5,84586E-09	16	1,78299E-08	-1,1984E-08
5,98694E-09	15,7	1,81706E-08	-1,21836E-08
6,09568E-09	15,7	1,81706E-08	-1,20749E-08
6,17494E-09	14,9	1,91462E-08	-1,29713E-08
6,08917E-09	15,7	1,81706E-08	-1,20814E-08
6,16151E-09	15,6	1,8297E-08	-1,21255E-08

1 point removed			
mean	STD	%STD	
-1,209E-08	7,34239E-11	0,607317	

		Migration time	Area	C. Area	mean	STD	%STD
L-ASP	1	49,9	15412	3,345959	4,295696	0,697054	16,22717
	2	48,7	19938	4,435216			
	3	47,85	18995	4,300505			
	4	47,2	17436	4,001907			
	5	47,85	24225	5,484587			
	6	47,25	18342	4,205397			

1 point removed			
mean	STD	%STD	
4,485622	0,580355	12,9384	

migration time			
mean	STD	%STD	
48,125	1,025061	2,129397	

apparent mobility	EOF time	mobility EOF	mobility
5,71639E-09	16	1,78299E-08	-1,21129E-08
5,85786E-09	15,7	1,81706E-08	-1,23127E-08
5,96192E-09	15,7	1,81706E-08	-1,22086E-08
6,04402E-09	14,9	1,91462E-08	-1,31021E-08
5,96192E-09	15,7	1,81706E-08	-1,22088E-08
6,03762E-09	15,6	1,8287E-08	-1,22494E-08

1 point removed			
mean	STD	%STD	
-1,2218E-08	7,27681E-11	0,595559	

8.2 Linearity

High end

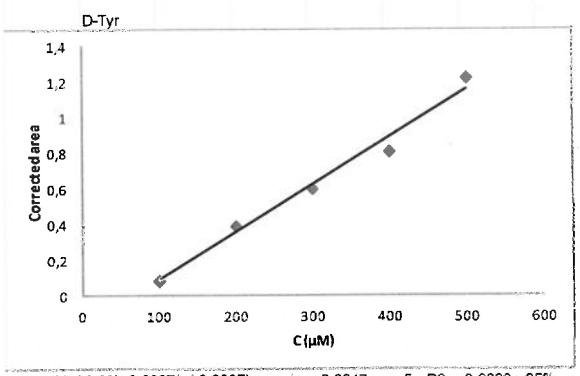

y=-0.19(+/-0.22)+0.0027(+/-0.0007)x ; sy/x = 0.0647; n = 5 ; R2 = 0,9830 ; 95%

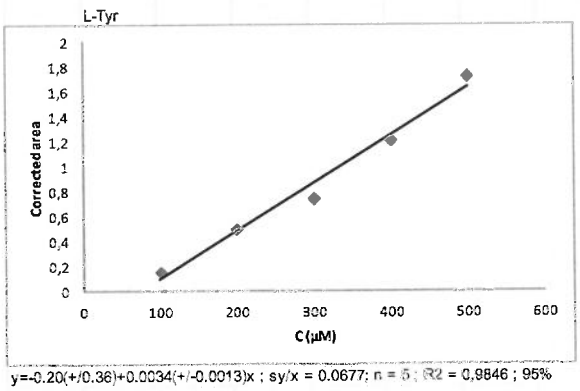

y=-0.20(+/-0.36)+0.0034(+/-0.0013)x ; sy/x = 0.0677; n = 5 ; R2 = 0,9846 ; 95%

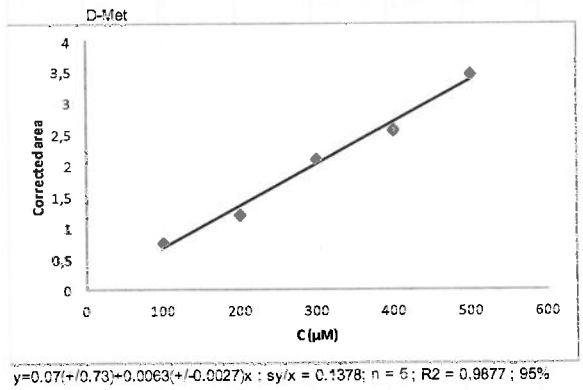

y=0.07(+/-0.73)+0.0063(+/-0.0027)x ; sy/x = 0.1378; n = 5 ; R2 = 0,9877 ; 95%

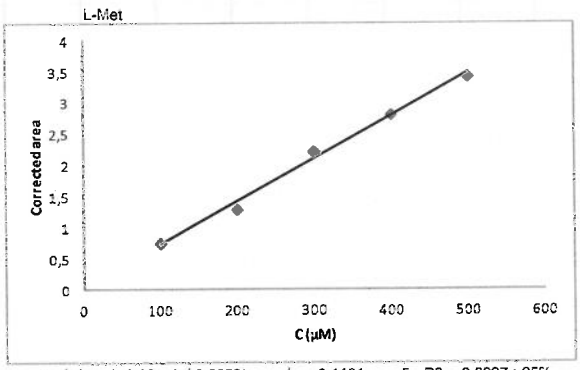

y=-0.02(+/-0.62)+0.0071(+/-0.0023)x ; sy/x = 0.1191; n = 5 ; R2 = 0.9927 ; 95%

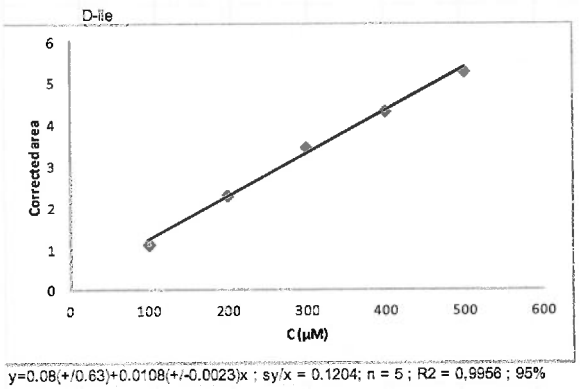

y=0.08(+/-0.63)+0.0108(+/-0.0023)x ; sy/x = 0.1204; n = 5 ; R2 = 0,9956 ; 95%

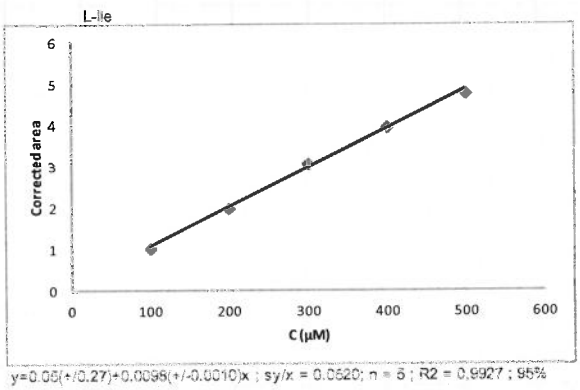

y=0.06(+/-0.27)+0.0096(+/-0.0010)x ; sy/x = 0.0520; n = 5 ; R2 = 0,9927 ; 95%

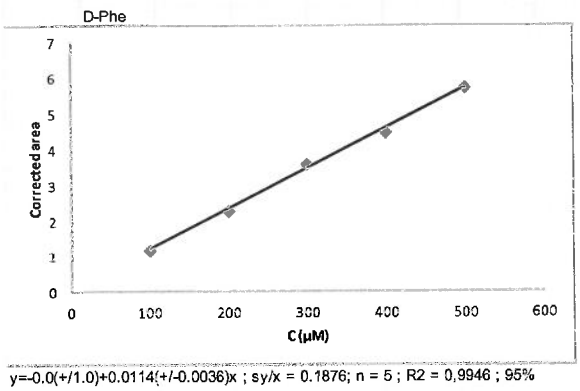

y=-0.0(+/-1.0)+0.0114(+/-0.0036)x ; sy/x = 0.1876; n = 5 ; R2 = 0,9946 ; 95%

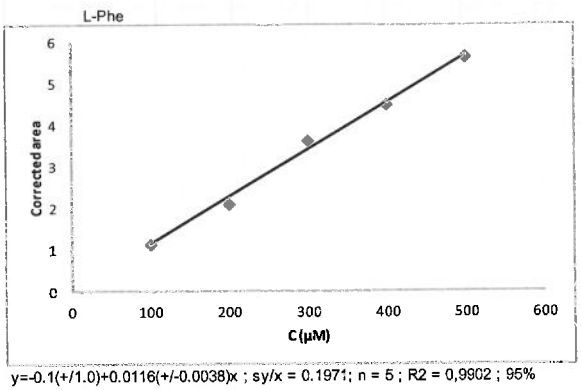

y=-0.1(+/-1.0)+0.0116(+/-0.0038)x ; sy/x = 0.1971; n = 5 ; R2 = 0,9902 ; 95%

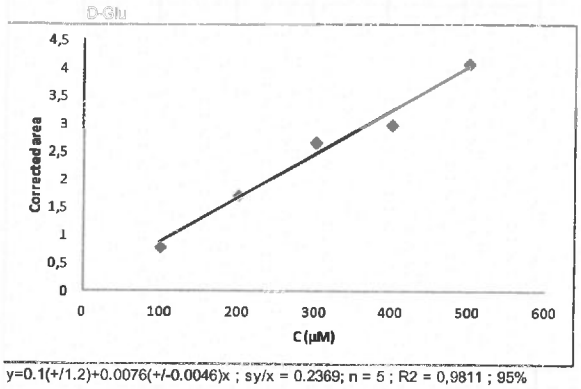

y=0.1(+/1.2)+0.0076(+/-0.0046)x ; sy/x = 0.2369; n = 5 ; R2 = 0,9811 ; 95%

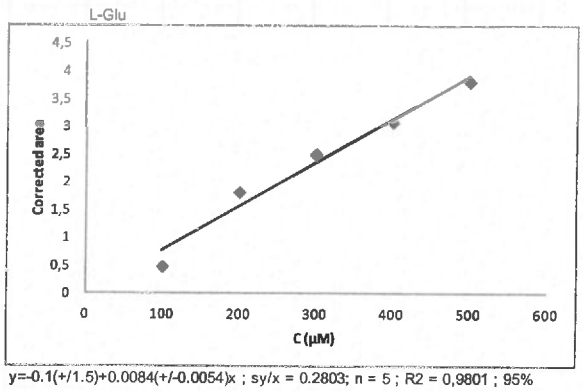

y=-0.1(+/1.5)+0.0084(+/-0.0054)x ; sy/x = 0.2803; n = 5 ; R2 = 0,9801 ; 95%

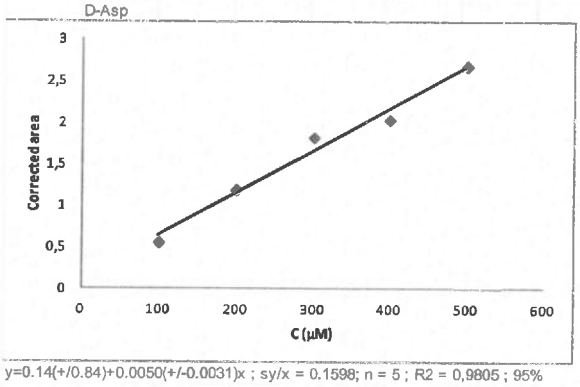

y=0.14(+/0.84)+0.0050(+/-0.0031)x ; sy/x = 0.1598; n = 5 ; R2 = 0,9805 ; 95%

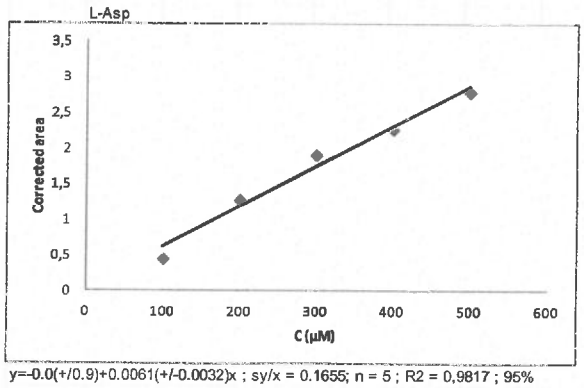

y=-0.0(+/0.9)+0.0061(+/-0.0032)x ; sy/x = 0.1655; n = 5 ; R2 = 0,9817 ; 95%

	Filename		Migration time	Area	total concentration (uM)	C. Area
D-TYR	150522 01	1	30,95	3491	500	1,221943996
	150522 03	2	29,8	2224	400	0,808501119
	150522 04	3	29,45	1626	300	0,598132428
	150522 05	4	28,75	1035	200	0,39
	150522 06	5	28,95	225	100	0,084196891

		Migration time	Area	total concentration (uM)	C. Area
L-TYR	1	32,1	5103	500	1,722196262
	2	30,9	3458	400	1,212351672
	3	30,5	2091	300	0,742704918
	4	29,75	1365	200	0,497058824
	5	30	425	100	0,153472222

		Migration time	Area	total concentration (uM)	C. Area
D-MET	1	33,35	10646	500	3,45822089
	2	32,15	7616	400	2,566303784
	3	31,75	6165	300	2,103543307
	4	31	3461	200	1,209489247
	5	31,25	2180	100	0,755733333

		Migration time	Area	total concentration (uM)	C. Area
L-MET	1	34,25	10807	500	3,418272506
	2	33	8547	400	2,805833333
	3	32,6	6681	300	2,220168712
	4	31,8	3770	200	1,28432914
	5	32,05	2202	100	0,744305772

		Migration time	Area	total concentration (uM)	C. Area
D-ILE	1	35,35	17189	500	5,267727487
	2	34,05	13553	400	4,312016642
	3	33,65	10701	300	3,445096582
	4	32,8	6909	200	2,281935976
	5	33,05	3348	100	1,097428139

		Migration time	Area	total concentration (uM)	C. Area
L-ILE	1	37,6	16506	500	4,755718085
	2	36,15	13158	400	3,943153527
	3	35,7	10056	300	3,051540616
	4	34,8	6360	200	1,979885057
	5	35,05	3336	100	1,031098431

		Migration time	Area	total concentration (uM)	C. Area
D-PHE	1	40,65	21515	500	5,733804838
	2	38,95	16067	400	4,468784767
	3	38,5	12729	300	3,581753247
	4	37,5	7817	200	2,258244444
	5	37,8	4055	100	1,162147266

		Migration time	Area	total concentration (uM)	C. Area
L-PHE	1	43	22395	500	5,642151163
	2	41,15	17073	400	4,494714459
	3	40,7	13637	300	3,629832105
	4	39,6	7686	200	2,102651515
	5	39,9	4203	100	1,141165414

		Migration time	Area	total concentration (uM)	C. Area
D-GLU	1	45,55	17220	500	4,095499451
	2	44	12212	400	3,006742424
	3	43,45	10742	300	2,678289221
	4	42,15	6669	200	1,71405694
	5	42,35	3077	100	0,787111373

		Migration time	Area	total concentration (uM)	C. Area
L-GLU	1	47,65	16779	500	3,814742917
	2	45,95	13038	400	3,073884657
	3	45,35	10456	300	2,497758177
	4	43,95	7374	200	1,817633675
	5	44,1	1984	100	0,487377173

		Migration time	Area	total concentration (uM)	C. Area
D-ASP	1	48,8	12062	500	2,677698087
	2	47,1	8826	400	2,030042463
	3	46,5	7782	300	1,813010753
	4	45,05	4950	200	1,190344062
	5	45,2	2325	100	0,557245575

		Migration time	Area	total concentration (uM)	C. Area
L-ASP	1	49,85	12807	500	2,783199599
	2	48,1	10022	400	2,257207207
	3	47,45	8339	300	1,903881279

Low end

D-Met

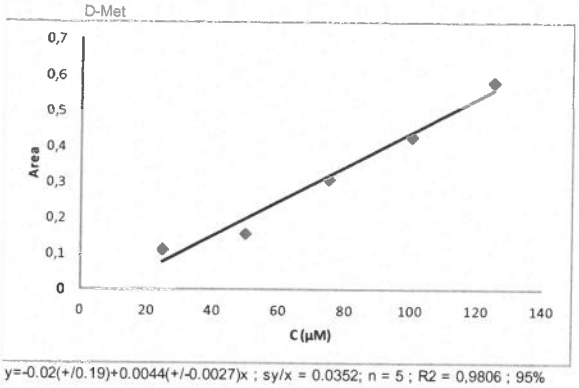

y=-0.02(+/0.19)+0.0044(+/-0.0027)x ; sy/x = 0.0352; n = 5 ; R2 = 0,9806 ; 95%

L-Met

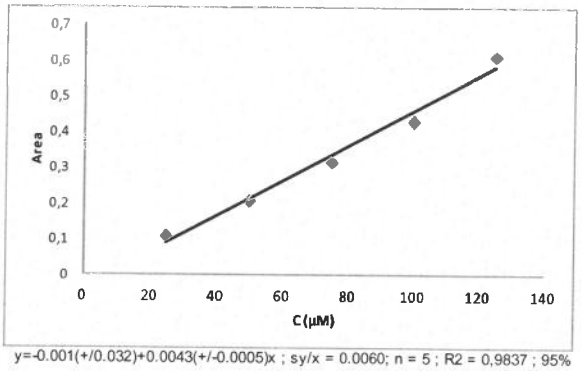

y=-0.001(+/0.032)+0.0043(+/-0.0005)x ; sy/x = 0.0060; n = 5 ; R2 = 0,9837 ; 95%

D-Ile

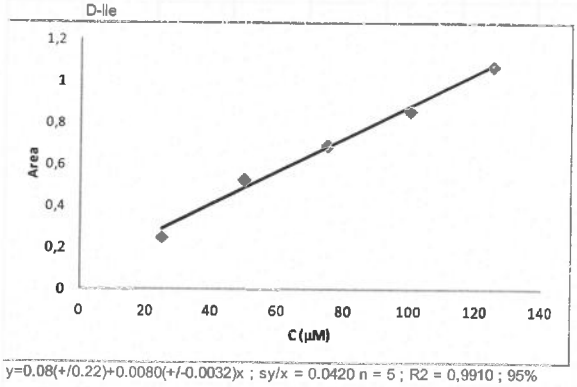

y=0.08(+/0.22)+0.0080(+/-0.0032)x ; sy/x = 0.0420 n = 5 ; R2 = 0,9910 ; 95%

L-Ile

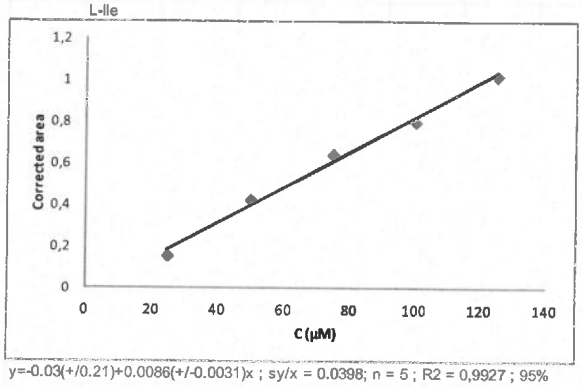

y=-0.03(+/0.21)+0.0086(+/-0.0031)x ; sy/x = 0.0398; n = 5 ; R2 = 0,9927 ; 95%

D-Phe

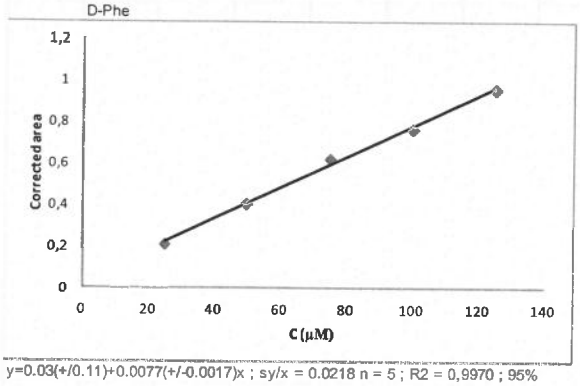

y=0.03(+/0.11)+0.0077(+/-0.0017)x ; sy/x = 0.0218 n = 5 ; R2 = 0,9970 ; 95%

L-Phe

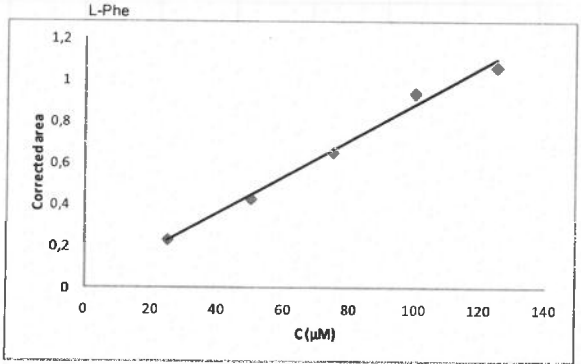

y=-0.02(+/0.17)+0.0094(+/-0.0025)x ; sy/x = 0.0318; n = 5 ; R2 = 0,9902 ; 95%

D-Glu

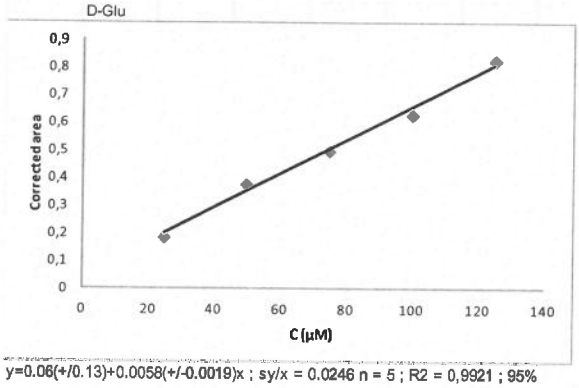

y=0.06(+/0.13)+0.0058(+/-0.0019)x ; sy/x = 0.0246 n = 5 ; R2 = 0,9921 ; 95%

L-Glu

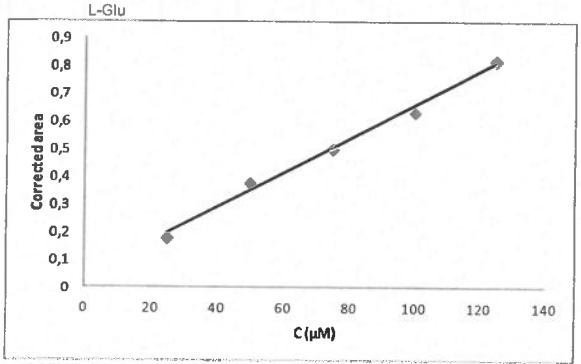

y=0.05(+/0.15)+0.0059(+/-0.0022)x ; sy/x = 0.0285 n = 5 ; R2 = 0,9917 ; 95%

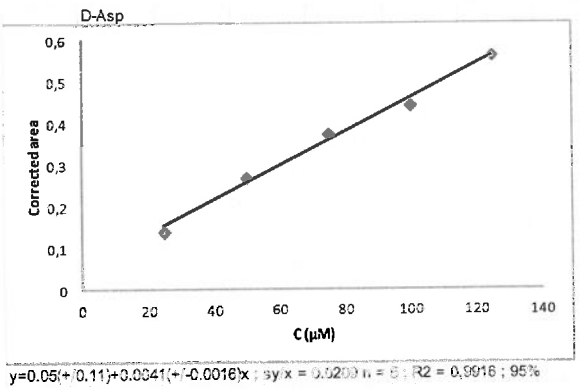

y=0.05(+/-0.11)+0.0041(+/-0.0016)x ; sy/x = 0.0200 n = 5 ; R2 = 0.9916 ; 95%

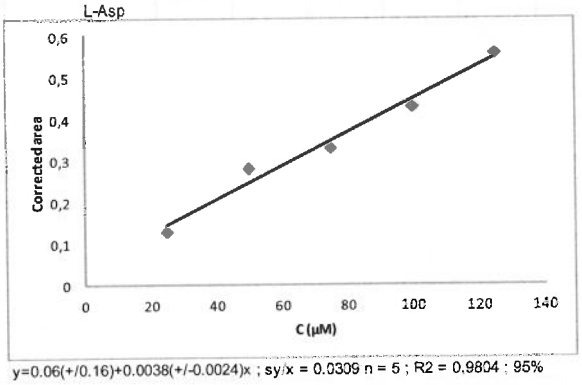

y=0.06(+/0.16)+0.0038(+/-0.0024)x ; sy/x = 0.0309 n = 5 ; R2 = 0.9804 ; 95%

	Filename		Migration time	Area	total concentration (uM)	C. Area
D-TYR	150527 06	1	27,9	111	125	0,043100358
	150527 01	2	29,75	372	100	0,135462185
	150527 02	3	28,85	354	75	0,132928943
	150527 03	4			50	#DIV/0!
	150527 04	5			25	#DIV/0!

		Migration time	Area	total concentration (uM)	C. Area
L-TYR	1	28,6	453	125	0,171590909
	2	30,95	926	100	0,324124933
	3	29,95	539	75	0,194963829
	4			50	#DIV/0!
	5	30,5	150	25	0,053278689

		Migration time	Area	total concentration (uM)	C. Area
D-MET	1	29,75	1598	125	0,581904762
	2	32,2	1272	100	0,427950311
	3	31,15	890	75	0,30952381
	4	30,95	446	50	0,156112009
	5	31,3	327	25	0,113178914

		Migration time	Area	total concentration (uM)	C. Area
L-MET	1	30,5	1725	125	0,612704918
	2	33,05	1317	100	0,431694402
	3	31,95	933	75	0,316353678
	4	31,8	612	50	0,208490566
	5	31,6	321	25	0,110047468

		Migration time	Area	total concentration (uM)	C. Area
D-ILE	1	31,6	3132	125	1,073734177
	2	34,25	2725	100	0,861922141
	3	33,15	2123	75	0,69379085
	4	32,95	1605	50	0,527693475
	5	32,4	753	25	0,251774691

		Migration time	Area	total concentration (uM)	C. Area
L-ILE	1	33,4	3159	125	1,024625749
	2	36,4	2682	100	0,798214286
	3	35,15	2079	75	0,640753912
	4	34,95	1374	50	0,425894134
	5	34,35	494	25	0,155798156

D-PHE

	Migration time	Area	total concentration (uM)	C. Area
1	36,2	3205	125	0,959139042
2	39,75	2820	100	0,768553459
3	38,2	2189	75	0,620789703
4	38	1424	50	0,405964912
5	37,3	723	25	0,209986595

L-PHE

	Migration time	Area	total concentration (uM)	C. Area
1	38,2	3762	125	1,066884817
2	42,15	3650	100	0,938117833
3	40,4	2435	75	0,65294967
4	40,2	1587	50	0,427674129
5	39,45	843	25	0,231495564

D-GLU

	Migration time	Area	total concentration (uM)	C. Area
1	39,55	3011	125	0,824757691
2	43,5	2531	100	0,63032567
3	41,9	1916	75	0,495385839
4	41,75	1458	50	0,378323353
5	40,95	708	25	0,187301587

L-GLU

	Migration time	Area	total concentration (uM)	C. Area
1	41,1	3120	125	0,822384428
2	45,35	2642	100	0,631128262
3	43,65	2022	75	0,501832761
4	43,45	1520	50	0,37897967
5	42,65	702	25	0,178311841

D-ASP

	Migration time	Area	total concentration (uM)	C. Area
1	42,1	2182	125	0,561480602
2	46,5	1896	100	0,44172043
3	44,75	1539	75	0,372569832
4	44,6	1098	50	0,266704036
5	43,75	561	25	0,138914286

L-ASP

	Migration time	Area	total concentration (uM)	C. Area
1	42,95	2211	125	0,557683353
2	47,5	1883	100	0,42945614
3	45,65	1391	75	0,330102227
4	45,5	1185	50	0,282142857
5	44,65	536	25	0,130048526